

**BEST
POSSIBLE
SCAN**

AD/A-003 419

PULSED PLASMA PROPULSION TECHNOLOGY

Dominic J. Palumbo, et al

Fairchild Republic Company

Prepared for:

Air Force Rocket Propulsion Laboratory

July 1974

DISTRIBUTED BY:

NTIS

**National Technical Information Service
U. S. DEPARTMENT OF COMMERCE**

REPORT DOCUMENTATION PAGE		READ INSTRUCTIONS BEFORE COMPLETING FORM
1. REPORT NUMBER AFRPL-TR-74-50	2. GOVT ACCESSION NO.	3. RECIPIENT'S CATALOG NUMBER AD/A-CO3419
4. TITLE (and Subtitle) Pulsed Plasma Propulsion Technology		5. TYPE OF REPORT & PERIOD COVERED Interim May 1973 thru Jul 1974
		6. PERFORMING ORG. REPORT NUMBER
7. AUTHOR(s) Dominic J. Palumbo William J. Guman Martin Begon		8. CONTRACT OR GRANT NUMBER(s) F04611-72-C-0053
9. PERFORMING ORGANIZATION NAME AND ADDRESS Fairchild Industries, Inc. Fairchild Republic Company Farmingdale NY 11735		10. PROGRAM ELEMENT, PROJECT, TASK AREA & WORK UNIT NUMBERS 6230 2F 3058 305812
11. CONTROLLING OFFICE NAME AND ADDRESS Air Force Rocket Propulsion Laboratory Edwards CA 93523		12. REPORT DATE
		13. NUMBER OF PAGES 86
14. MONITORING AGENCY NAME & ADDRESS (if different from Controlling Office) Same as "11" above		15. SECURITY CLASS. (of this report) Unclassified
		15a. DECLASSIFICATION DOWNGRADING SCHEDULE
16. DISTRIBUTION STATEMENT (of this Report) Approved for Public Release, Distribution Unlimited		
17. DISTRIBUTION STATEMENT (of the abstract entered in Block 20, if different from Report) Same as "16" above		
18. SUPPLEMENTARY NOTES None		
19. KEY WORDS (Continue on reverse side if necessary and identify by block number) Space Propulsion, Electric Propulsion, Plasma Propulsion, Solid Propellant, Capacitor Discharge, ARC Discharge		
20. ABSTRACT (Continue on reverse side if necessary and identify by block number) An engineering prototype pulsed plasma propulsion system delivering 1mb (4.45mN) of thrust at a specific impulse of 1794s and having a total impulse capability of 38,284 lb-s (166,00Ns) has been designed and completely fabricat- ed. The thrust efficiency is 31.5% and the overall system efficiency is 25.3%. The system, including structure, capacitors, breadboard power converter and propellant weighs 50.231b (22.8kg). Solid Teflon propellant is stored in the shape of a helical coil to meet volumetric constraints (the total volume		

UNCLASSIFIED

SECURITY CLASSIFICATION OF THIS PAGE(When Data Entered)

required to house the system is 1.36 cu ft.). Two inputs are required to operate the system; a 28VDC supply of power capable of producing 154.5W for 1mlb of thrust and an SCR triggering pulse. The system will provide discrete impulse bits 6mlb-s (26.6mNs) in amplitude in a period of 15 microseconds and may be used in a single shot on command or continuous operation mode. Thermal and radiated radio frequency interference compatibility tests were done. Radiated RF measurements indicated that all noise produced by the arc occurs at the instant the arc is struck. The duration of the noise spike at initiation is from 100 to 300 nanoseconds with a rise time of the order of 10ns. The magnitude follows a normal distribution and is therefore more or less random. Moreover, the maximum amplitude of the radiated noise spike was shown to be dependent only on the initial voltage across the electrode gap (a power law dependency on voltage to the 3.687) and independent of the energy stored in the capacitor bank. Narrow band measurements indicated impulse type noise (flat frequency spectrum) from 23 to 12.4 GHz. The average value of the Poynting flux at the 2740VDC thruster operating voltage over this range is .0141mW/m²/MHz. A thruster life-test was initiated but not accomplished due to persistent oil leakage from the energy storage capacitors. In order to endurance test the thruster system it will be necessary to rebuild the four 60 microfarad capacitors incorporating state-of-the-art techniques to insure a hermetic seal and eliminate oil leakage.

UNCLASSIFIED

SECURITY CLASSIFICATION OF THIS PAGE(When Data Entered)

ia

TABLE OF CONTENTS

<u>Section</u>	<u>Page</u>
I INTRODUCTION	1
II THRUSTER SYSTEM DESIGN AND DESCRIPTION	5
1. Electrode/Propellant Geometry	5
2. Discharge Initiation Circuitry	6
3. Power Converter	7
4. Energy Storage Capacitors	13
5. Propellant Feed System	16
a. Storage Geometry	16
b. Preliminary Propellant Feed Tests	17
c. Results of Preliminary Testing	22
d. Propellant Support Structure and Helical Feed System	27
III RESULTS OF THERMAL-VACUUM AND PERFORMANCE TESTS	31
1. Thermal Vacuum Tests	31
2. Thruster Performance	36
IV PERFORMANCE OF THRUSTER SYSTEM	41
V RESULTS OF RFI TESTING	47
1. General	47
2. Experimental Set-Up and Equipment	47
3. Measurement Results	53
a. Description of Data and Recording Technique	53
b. RF Pattern Measurements	55
c. Data Reduction	58
d. Narrow Band Data	58
e. Broad Band Data	59
f. Dependence of RF Emission on Voltage	59
4. Possible Effects of Environment on Measured Radiated RF	63
VI SAFETY CONSIDERATIONS	65
VII CONCLUSIONS AND RECOMMENDATIONS	67
REFERENCES	70
APPENDIX A	A - 1
APPENDIX B	B - 1

NOTICE

When Government drawings, specifications, or other data are used for any purpose other than in connection with a definitely related Government procurement operation, the United States Government thereby incurs no responsibility nor any obligation whatsoever; and the fact that the Government may have formulated, furnished, or in any way supplied the said drawings, specifications, or other data, is not to be regarded by implication or otherwise as in any manner licensing the holder or any other person or corporation, or conveying any rights or permission to manufacture, use, or sell any patented invention that may in any way be related thereto.

FOREWORD

This interim report was prepared by Fairchild Industries, Inc., Fairchild Republic Company under Air Force Contract FO4611-72-C-0053, "Pulsed Plasma Propulsion Technology", MS147U200.

The research reported upon was supported by the Air Force Rocket Propulsion Laboratory. The program was monitored in the Liquid Rocket Division by Lt. Sharon Pruitt.

Work on this contract began in May 1973 and was completed in July 1974 and the pertinent studies of this period are reported herein. This report was submitted by the authors in July 1974.

The authors wish to acknowledge the significant contributions of Mr. John Muldoon and especially Mr. William Johnson and Mr. Stanley Pasternack in the Laboratory effort. Specific acknowledgement to Dr. K. Thomassen, as consultant, for his valuable contributions to the RFI testing phase of this program is made.

This technical report has been reviewed and is approved.


CHARLES E. SIEBER, Lt Colonel, USAF
Chief, Liquid Rocket Division

ACCESSION NO.	
NTIS	Write Section <input type="checkbox"/>
DDI	Dist. Section <input type="checkbox"/>
UNCLASSIFIED	<input type="checkbox"/>
JUSTIFICATION	
BY	
DISTRIBUTION/AVAILABILITY CODES	
Dist.	AVAIL. CODE/SP. CIAL
A	

ic

LIST OF ILLUSTRATIONS

<u>Figure</u>	<u>Page</u>
1. Electrode/Propellant Geometry	5
2. Schematic of Discharge Initiation Circuitry	6
3. Schematic of Power Converter	9
4. Basic Thruster Configuration	18
5. Schematic of Propellant Feed System Used for Preliminary Testing With Straight Rods	21
6. Prototype Nozzle Using Straight Propellant Rods	22
7. One Millipound Thruster System With Helical Solid Propellant Storage	30
8. Temperature Vs. Time at Various Locations on Thruster	32
9. Temperature Vs. Time Included Added Radiation Area	34
10. Thruster Nozzle After Performance Testing	38
11. Photographs of Thruster System	42
12. Capacitor Failure	43
13. Second Capacitor Failure	44
14. RF Measurement Set-Up	48
15. Broadband Detection System	49
16. Broadband Detection System Used for Narrow Band Measurements	49
17. Typical Thruster RF Pulse	50
18. Schematic of Pulse Amplifier	50
19. Gain Vs. Frequency of Pulse Amplifier	50
20. Schematic of Measurement Set-Up	52
21. Exhaust Cone Geometry	53
22. Cumulative Frequency Vs. RF Data Level	54
23. Pattern Measurements to Determine Scattering Effects of Glass Tube	55
24. Schematic of Pattern Measurement Set-Up	56
25. Thruster RF Pattern in the H-Plane	57
26. Frequency Spectrum of Radiated Poynting Flux	57
27. Poynting Flux Vs. Initial Voltage	61
28. Poynting Flux Vs. Initial Voltage and Energy	62

I. INTRODUCTION

The objective of this program was to design, fabricate and test a laboratory prototype solid propellant pulsed plasma propulsion system having the following characteristics:

- (i) a thrust of one millipound (4.45mN);
- (ii) a specific impulse of 1500s;
- (iii) a maximum average required power of 137W;
- (iv) a total impulse capability of 37,500 lb-s (155,875Ns);
- (v) a total system design weight of 45 lbs (20.4 kg);
- (vi) a total design volume of 1.5 ft³ (.0425 m³).

After fabrication, the thruster was to be placed on life test in a vacuum (10^{-5} torr) and operated until 10,000 lb-s (44,500Ns) of total impulse was generated before the system was to be delivered to the Air Force Rocket Propulsion Laboratory for completion of the remaining total impulse capability at their facility. Besides this performance demonstration, radiated radio frequency and conductive electromagnetic interference testing, as well as thermal vacuum testing was to be done at Fairchild Republic.

The first phase of this program, i. e., the development and design of the electrode/propellant nozzle configuration yielding 30% thrust efficiency ($T^2/2inP$) at 1500s specific impulse (power/thrust = 111 kw/mlb = 24.8 kw/mN), was successfully completed and reported in [1]. Teflon propellant in a side-feed configuration with parallel rail electrodes spaced 3 inches (7.62cm) apart and a total exposed propellant surface area of 7.8 in² (50.3 cm²) was found to be optimal to the best of our knowledge at a discharge energy of 750J. These conditions were the basic inputs for the design of the thruster system.

It was apparent at the onset of this program that if the objectives were to be achieved several areas of new technology would have to be incorporated into the system. These areas of technology are new in the sense that the associated hardware had never been tested at Fairchild Republic on a thruster in a vacuum prior to this program and that the qualification of each component would represent a major step forward in overall thruster system development.

The first major area of development was to demonstrate successful feeding of the solid propellant into the interelectrode gap from the sides since it was not necessary to feed propellant rods in this geometry during the performance demonstration phase of this program. Furthermore, in order to meet the volumetric constraint with the required 25 pounds (11.36 kg) of propellant, it would be necessary to store the rods in the shape of two helical coils; one fed into each side of the interelectrode gap. Although a circular section of propellant had been fed previously for a total of 1200 lb-s (53,400 Ns) on a 20J thruster, [2], no attempt at feeding a helical rod had been made until this program began.

The second area of advanced technology to be incorporated in the design of this thruster system involved the use of high energy density storage capacitors capable of at least 5.6 million discharges. A minimum requirement of 40J/lb (88J/kg) would be essential if the thruster design weight was to be achieved. Capacitors having this energy density were produced on a separate Air Force supported program [3] by Capacitor Specialists, Inc. (CSI). This high energy density was achieved by using a relatively recent developed dielectric called KF-film (polyvinylidene fluoride) in combination with paper and castor oil impregnant. Although prototype units had been fabricated at CSI for testing purposes and design life could be extrapolated to many million discharges there was some speculation at the onset of this program as to whether or not such capacitors would have an energy delivery efficiency compatible with that of the Mylar dielectric units used to demonstrate the performance goal. This speculation arose because the dissipation factor associated with KF-film is about three times that of Mylar at the thruster discharge frequency (roughly 10^5 Hz). In conjunction with this peculiarity it was also questionable as to whether or not the capacitor temperature could be kept below the 45°C value required for long life without adding excessively heavy cooling structure to the thruster. Cooling structure, in effect, would reduce the savings in weight derived from using high energy density units.

Power converters using the "fly-back" technique for capacitor charging from a DC source had been procured by Fairchild Republic for use on pulsed plasma thrusters on previous programs. The maximum input power of these units was 25W and the maximum high voltage output was 1.5 kV. Since the optimum energy density of KF-film capacitors occurs at 2.5 kV, the power converter used on this program would have to deliver this higher voltage so that minimum capacitor weight could be assured.

Moreover, a minimum energy delivery rate of 111 J/s would be necessary to produce the 1 mlb of thrust with a maximum power input of 137W to the converter. This condition required a minimum power conversion efficiency of 81.2%. We were assured by Wilmore Electronics, the vendor who would build the power converter, that a minimum efficiency of 82% could be guaranteed at an output voltage of 2.5 kV. The final area of new technology therefore, would be design and fabrication of a breadboard converter having the above characteristics to be used with the thruster and evaluated along with the overall system.

II. THRUSTER SYSTEM DESIGN AND DESCRIPTION

1. ELECTRODE/PROPELLANT GEOMETRY

The choice of a particular electrode/propellant geometry is generally dictated by the thruster performance level sought. In order to generate the desired performance of 30% thrust efficiency at 1500s specific impulse an evaluation of various configurations was carried out in the first phase of this program. The results of that study were presented in Ref. 1, and on the basis of those results the side-fed parallel rail electrode/propellant configuration with the following pertinent dimensions was selected:

- (i) Interelectrode spacing = 3 in. (7.62 cm)
- (ii) Exposed propellant area = 7.8 in.² (50.3 cm²)
- (iii) Spacing between propellant rods = 0.3 in. (7.62 mm)
- (iv) Electrode width = 1.5 in. (4.27 cm)
- (v) Electrode length = 1.6 in. (4.52 cm)

This geometric arrangement is depicted schematically in Figure 1.

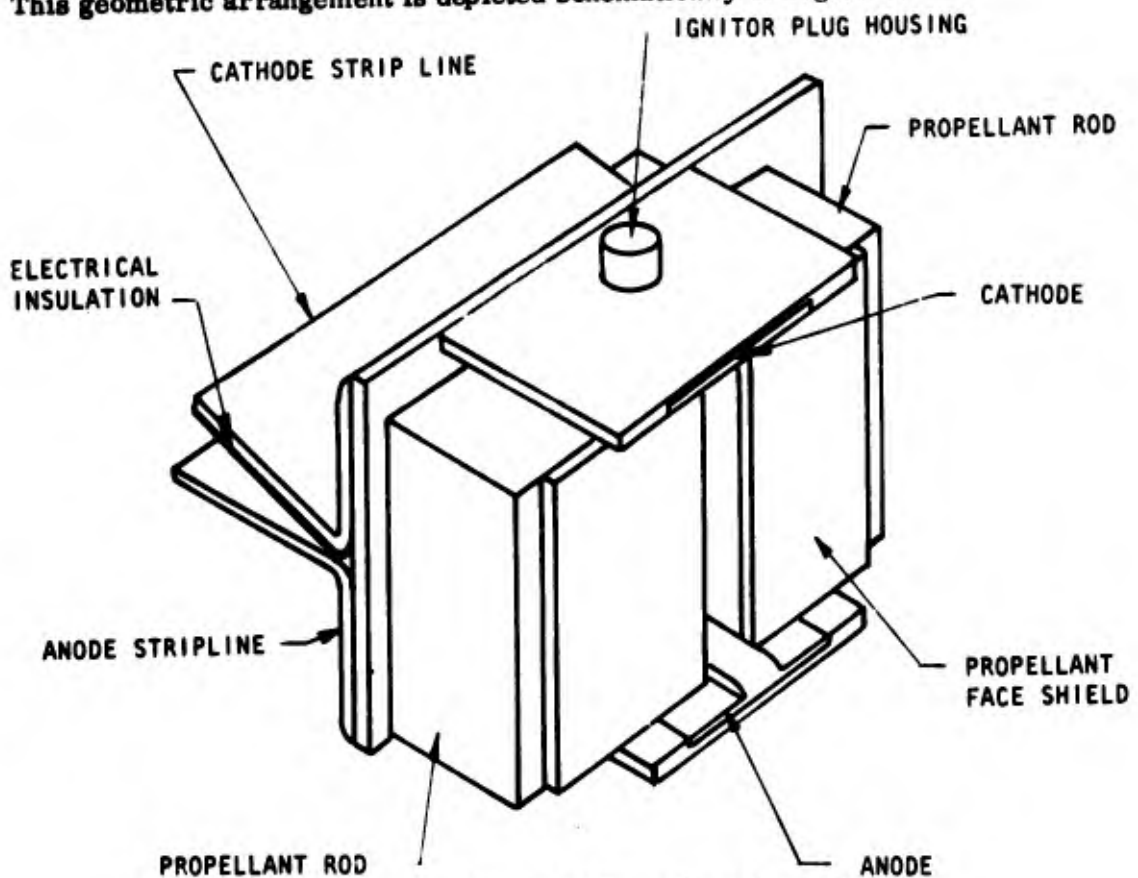


Figure 1. Electrode/Propellant Geometry

Electrodes and strip lines are fabricated from oxygen free copper. An exhaust cone surrounds the electrodes to suppress backward propagation of radiated radio frequency and plasma particles. This cone is a triangular prism with sides inclined to the horizontal 30°. The cone is fabricated using .125 in. (3.17 mm) Mykroy 1100 high temperature ceramic sheet with .01 in. (.254 mm) oxygen free copper cemented to the exterior surfaces and soft soldered at the seams. The surrounding copper is grounded (i.e., electrically connected to the thruster cathode) to provide an electromagnetic shield. An insulating coating of Magna-X500 potting compound applied to the exposed copper surface eliminates the possibility of the plasma electrically coupling to ground through the copper shield.

Fabrication details on the insulation components (i.e., face shield, backplate, etc.) will be discussed in more detail in subsection 5 of this section.

2. DISCHARGE INITIATION CIRCUITRY

The circuitry used to initiate discharge of the main capacitor bank is the same as that which has been used at Fairchild Republic for the past several years. A circuit schematic is shown below in Figure 2.

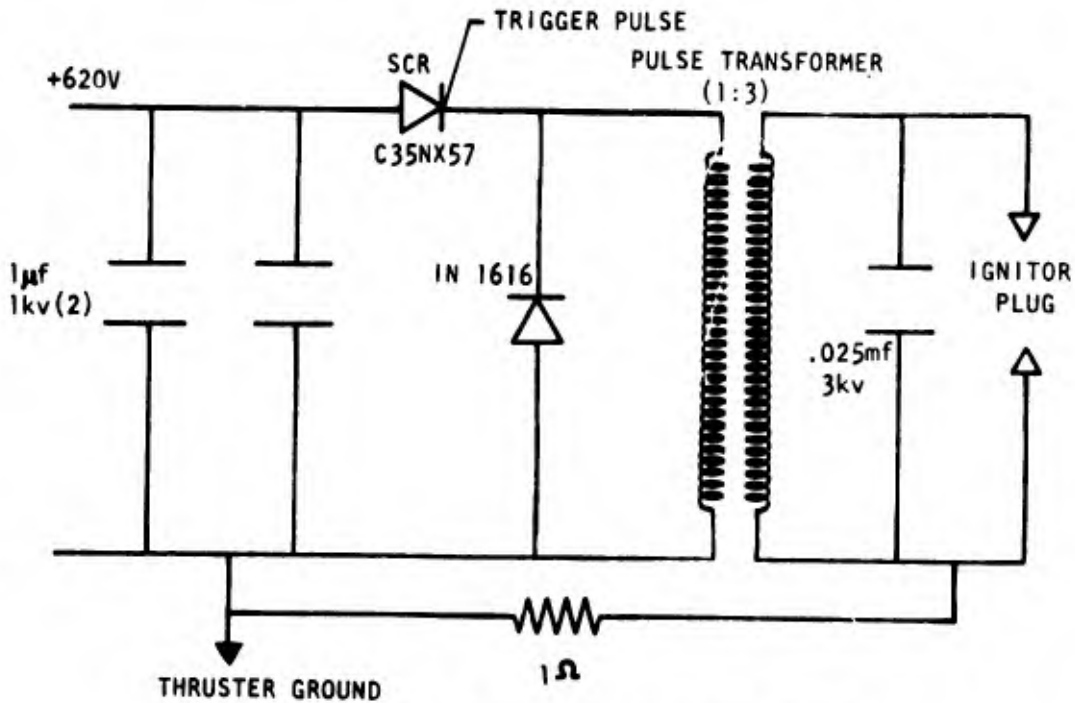


Figure 2. Schematic of Discharge Initiation Circuitry

Electrical breakdown between the electrodes in vacuum is initiated by a microdischarge generated at the surface of a solid state igniter plug. This process produces a microscopic amount of ionized debris which generates the initial streamer causing current to flow between the electrodes from the main capacitor bank. The subsequent ablation of Teflon propellant provides the primary source of ionized particles once the arc is developed.

A thruster discharge is initiated by firing the SCR which causes the two one microfarad capacitors, which are charged to about 620 VDC, to dump their energy across the 1:3 stepup pulse transformer. The voltage buildup on the .025 microfarad capacitor on the secondary side appears simultaneously across the anode and cathode of the igniter plug and, upon reaching a sufficiently high value, causes a spark at the surface of the plug's semiconductor. The igniter plug is placed about .25 inches (6.35 mm) above the surface of the thruster cathode in a divergent circular channel machined from Mykroy 1100 ceramic. There is a hole approximately .25 inches (6.35 mm) in diameter drilled into the cathode through which the ionized particles produced by the igniter plug can pass into the interelectrode gap of the thruster electrodes. A one ohm resistor located between thruster ground and the plug cathode represents a high enough impedance with respect to the arc itself so that once breakdown occurs the arc will attach itself to the thruster cathode rather than remaining attached to the igniter plug cathode. This feature is important since severe erosion of the plug cathode would occur if the arc remained attached to it for any significant length of time. It is also for this reason that higher energy thrusters (> 100 J) do not have the plug pressed into the cathode as do the microthrusters built previously. The technique of physically isolating and locating the plug away from the surface of the thruster cathode evolved after several years of testing at higher energies.

3. POWER CONVERTER

The power converter was procured from Wilmore Electronics, Co., Inc. under Fairchild Republic specification MS147S0002 included in this report as Appendix A. Briefly, this specification calls for two voltage outputs from a 28 ± 2 VDC source. The 2500 V output was to be used on the 240 microfarad capacitor bank at a minimum charging rate of 111 J/s. A nominal 620 VDC output is used to charge the 2 microfarad capacitor bank in the discharge initiating (D.I.) circuit. These are the only two outputs required to operate the thruster.

The fly back technique for capacitor charging from a DC source is used. This technique consists of switching small amounts of magnetic energy across a transformer at a frequency high enough to generate appropriate output power. Thus, the output power is equal to $1/2 fLi^2$ where f is the frequency, L the transformer inductance, and i the average current during a single cycle. In the converter used on this thruster there are four separate channels providing power to the common high voltage output leads. Each channel operates at a frequency of 50 to 80 kHz. Switching elements sense the net output voltage and when the desired output voltage is achieved, the power to all channels is shut off, causing no more energy to be deposited. If the thruster is not triggered to discharge, the output voltage will remain on the capacitors and the converter will be in an "idle" state drawing from 4 to 6 W until thruster firing. Upon seeing the sudden drop in voltage on the output, the sensing circuitry turns on power to all channels once again and the charge cycle repeats itself. A schematic drawing of the power converter is included as Figure 3 of this report.

It is noted that the constraint of 137W maximum average input power and the required output of 111W to produce 1 millipound of thrust implies a conversion efficiency of about 82%. Wilmore Electronics assured Fairchild Republic that this efficiency could be achieved at the 2500V output but even higher efficiencies could be obtained at lower output voltages and conversely, a lower efficiency would result if the output voltage were higher. The efficiency of power conversion using the flyback technique falls off rapidly beyond the 1000V where 85 to 90% efficiency is state-of-the-art. This characteristic of the fly-back technique is made known at this time since it became necessary to increase the required output voltage above 2500 volts about two months after the program was initiated. The increase in output voltage came about because Capacitor Specialists, Inc., from whom the capacitors for this thruster were procured, came in out of specification on the low side by 10 microfarads per unit. Fairchild's specification called for four 60 microfarad $\pm 5\%$ units which would have yielded a total of 240 microfarads and given the necessary 750J energy level when charged to 2.5 kV. Instead, CSI informed Fairchild Republic just prior to delivery that the capacitors would only be 50 microfarads each. In order to generate 750J a voltage of 2.74 kV on 200 microfarads is needed. Fortunately, Wilmore had not begun to wind the transformers for the converter at the time this news was received and they were able to adjust their design to give this new output voltage at no extra cost to the program. Fairchild Republic was informed, however, that the

A

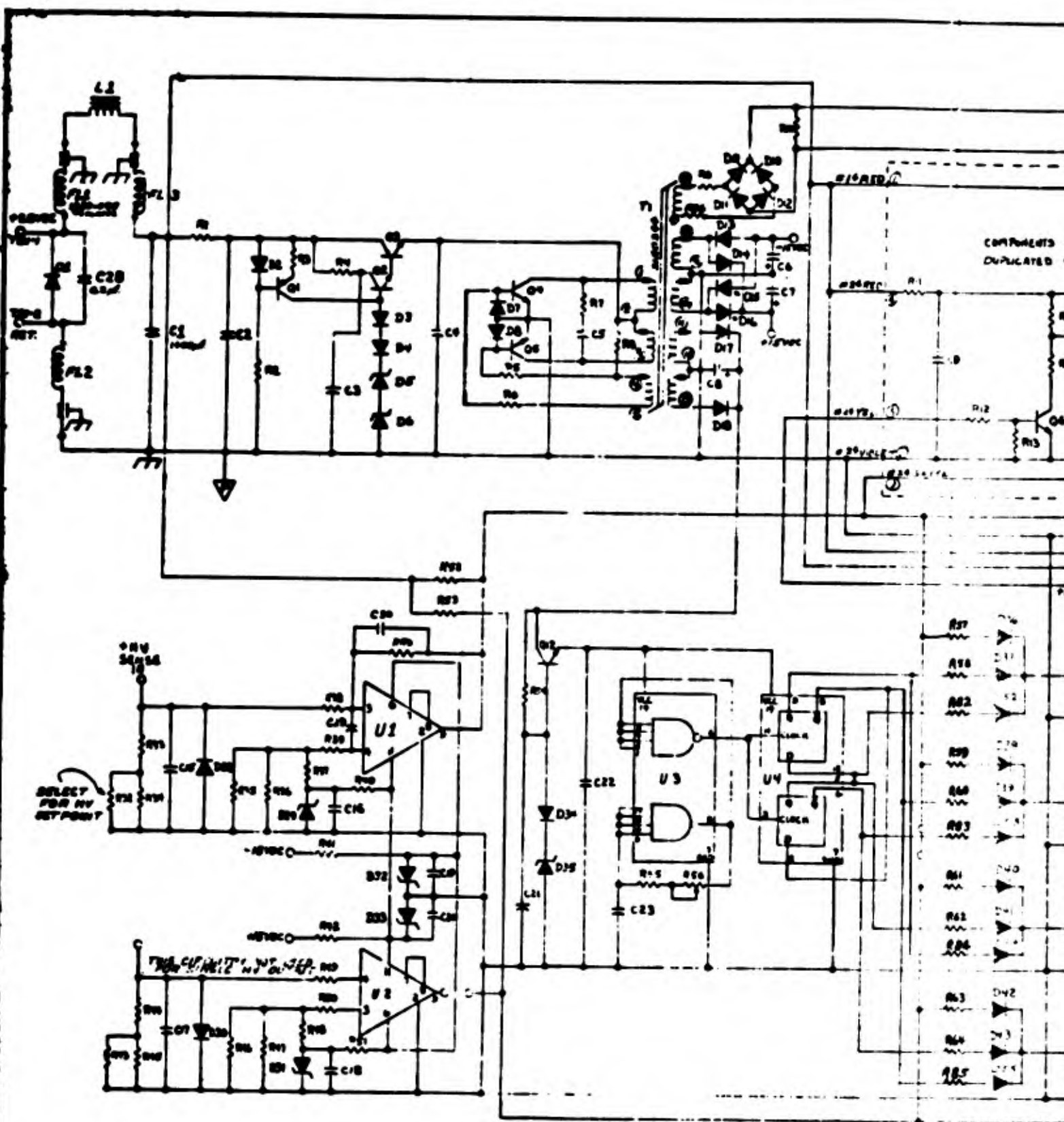
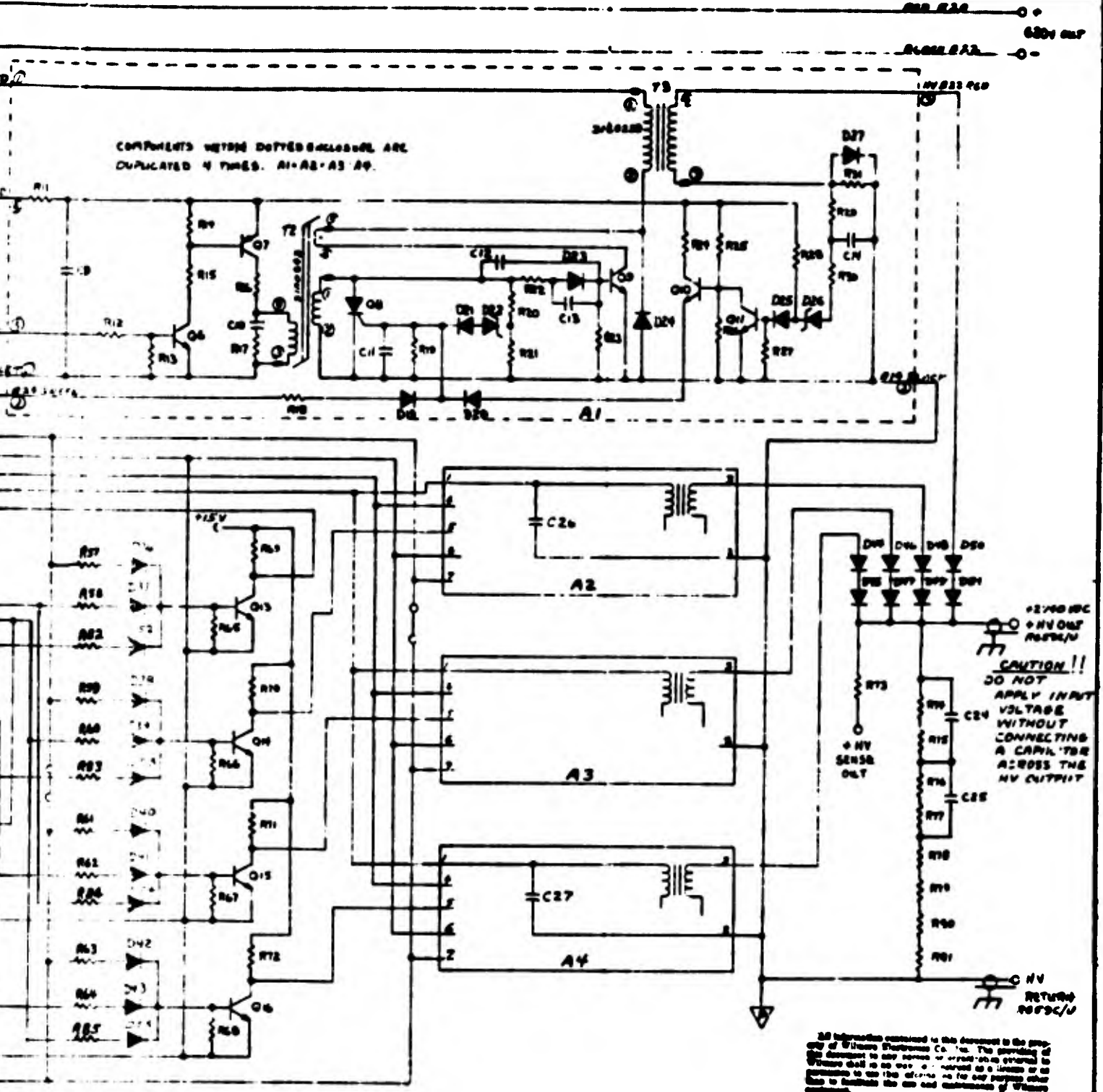


Figure 3. Schematic of Power Converter

B

REV	DATE	BY	CHKD

COMPONENTS WITHIN DOTTED LINES ARE
DUPLICATED 4 TIMES. A1-A3-A4



All information contained in this document is the property of Wilmore Electronics Co., Inc. The granting of this document to any person or organization is granted to that person or organization as a loan and is not to be used for any purpose other than to facilitate the design and construction of Wilmore equipment.

WILMORE ELECTRONICS CO., INC.	
RURALINDIA, N. CAROLINA	
MODEL	1216-1
SCHEMATIC DIAGRAM, III COLLE/SEC.	
3700V CAPACITOR 2MP/2 CANV	
DATE	16DEC67

74

17 August 1973

Capacitor Specialists, Inc.
P. O. Box 2052
Del Dios Highway
Escondido, California 92025

Attention: Mr Wayne White

Dear Wayne:

We will accept the six 50 microfarad capacitors even though they are out of spec (60 microfarads $\pm 5\%$) with the condition that the guaranteed lifetime of 6×10^6 discharges is met at 2740 volts as opposed to the 2500 volts originally specified. As I discussed with you over the phone, it will be necessary to go to 2740 volts, so that the discharge energy of 187.5 Joules per capacitor is maintained.

Sincerely,


Dominic J. Balumbo, Ph.D.
Project Engineer

DJP:mz

efficiency would come down two or three percent as a result of having to go to the higher voltage. This reduced efficiency was accepted since the alternative would have been to run at a discharge energy of 625J, and this would have decreased the specific impulse by two hundred seconds. The resultant drop in thrust efficiency would have been about 4.2 percent and the amount of propellant required to complete the required total impulse would have increased by 3.85 lbs (1.75kg). Increasing the required input power to 141W from 137W seemed the preferred approach. Hence, the final version of the converter delivers 2.74 kV at 80.4% conversion efficiency instead of 2.5 kV at 82%.

The breadboard converter was housed in a metal box measuring 8" x 10" x 2.6" (20.32 cm x 25.4 cm x 6.60 cm). The total weight was 4.75 lbs (2.16 kg). Test data supplied by Wilmore upon delivery of the unit is reproduced in Table 1. This data shows compliance with all aspects of our specification. The three data points at room temperature were verified at Fairchild Republic.

The efficiency of power conversion was measured by charging a 195 microfarad bank of CSI capacitors and recording the resultant voltage as a function of time on an oscilloscope. The average output power is then given as $\frac{1}{2} CV^2/\tau$ where C is the capacitance, V the final voltage and τ the elapsed time from zero charge to final charge on the capacitor bank. The input power during the charge cycle was obtained by simultaneously displaying input current and voltage as a function of time on an oscilloscope. The voltage was tapped at the input leads to the converter and fed directly into the scope. Current was measured by recording the voltage drop across a precalibrated .0175 ohm shunt in series with the ground lead to the converter. The time-averaged input power was then obtained by numerically integrating the product of current and voltage over the charge cycle using Simpson's rule and dividing by τ . The results of these calculations yielded an efficiency of 80.4% when the capacitor bank was charged to 2740 V.

In order to determine what the efficiency of the unit would be if the charge voltage were lowered to 2500 V, a series of tests were performed in which the efficiency was determined as a function of the ultimate voltage by interrupting the charge cycle at various times. The data obtained showed an almost linear increase in efficiency with decreasing ultimate voltage down to 1580V where an efficiency of 89.0% was measured. At 2065V the efficiency is 84.5% and at 1887V, 86.4%. Interpolating, one finds that at

TABLE 1. POWER CONVERTER TEST DATA

Input Voltage (V) Spec	Temperature (°C) Spec	Main Output Voltage (V) Spec	DI Voltage (V) Spec	Average Output Power (W) Spec
26 to 30	-17.8 to 60	2740 ± 2%	620	Minimum 111.1
26	-17.8	2739	609.3	129.1
26	+25	2737	616.5	120.5
26	+60	2723	621.25	114.5
28	-17.8	2739	609.6	132.1
28	+25	2737	616.8	123.2
28	+60	2723	621.46	119.4
30	-17.8	2739	609.8	138.7
30	+25	2737	617	128.9
30	+60	2723	621.66	124.9

2500V the efficiency would be 81.4% which is above the value of 81.2% required to generate one millipound of thrust at an average input power of 137W. Thus, if CSI had delivered the 240 microfarads of capacitance asked for, the required power conversion efficiency would have been obtained and an input power of 136.5W would have given one millipound. As it is, however, the 80.4% efficiency required 138.2W input at 2740V to generate the one millipound of thrust.

4. ENERGY STORAGE CAPACITORS

The requirement of 30% thrust efficiency at 1500s specific impulse was met during the first phase of this program [1] wherein a discharge energy of 750J was found necessary to produce this performance. A constraint of 20 lbs (9.11kg) on the basic thruster weight (i.e., less propellant) pretty much dictated the need for high energy density capacitors with a minimum of 40 J/lb (88 J/kg) deemed necessary. Energy storage capacitors having this energy density were produced in limited quantity by CSI under a separate AFRPL program [3]. This high energy density was realized by incorporating a dielectric film manufactured from polyvinylidene fluoride which is marketed by Kreha Corporation of America under the trade name KF-film. This film is unique in that its dielectric constant is much higher than that of other plastic films usually used in manufacturing capacitors. Research and development efforts at CSI showed that a composite dielectric system consisting of a layer of paper sandwiched between two layers of KF-film with a castor oil impregnant gave high energy density and long life. It was also found that maximum energy density and life expectancies of ten million discharges were obtainable at a voltage of 2.5 kV, which is optimal. In order to take advantage of this maximum energy density and produce a discharge energy of 750J a capacitance of 240 microfarads is required. For economical reasons CSI recommended that four capacitors, each having a capacitance of 60 microfarads be used to produce this capacitance.

The life requirement was calculated using an impulse/energy (thrust/power) ratio of 9.0 micropound-seconds/Joule (40.3 micronewtons/Joule). The impulse bit produced by a single thruster firing is then $9 \times 750 = 6750$ micropound-seconds. A total impulse of 37,500 pound-seconds therefore requires only $(37,500/6750) \times 10^6$ discharges or 5.58 million firings. At 30% thrust efficiency this number of firings would impart a total kinetic energy of 1,255 megajoules to the spacecraft. A design

life of ten million discharges with a guaranteed lifetime of six million was written into the procurement specification issued to CSI. This specification is included as Appendix B to this report. Six units were ordered from CSI to provide two spares, in case of early failures.

Approximately one week prior to the scheduled delivery date Fairchild Republic was informed that the capacitors would be 50 microfarads instead of 60 and that the units were ready to be shipped. The result of this change had a severe impact on the power conversion efficiency, as noted in the previous section. For program scheduling reasons it was not possible to reject the capacitors at that time so Fairchild accepted delivery with the understanding that even at 2740V the required pulse life would be met. This requirement was confirmed by CSI.

Upon receiving the units it was immediately obvious that CSI had not complied with specifications concerning the terminal geometry. The ground ring width and height were both completely out of specification, as well as the positive stud size and thread. In addition, the four threaded holes in the ground ring were off center as much as .06 inches (1.52 mm). Since the strip line collector plates for the thruster had already been fabricated to accommodate the capacitor geometry specified, and it was felt that no rework on the capacitor terminals should be done at Fairchild Republic, the units were sent back to CSI for modification to meet terminal specification requirements. This modification took approximately two weeks. When the units were received back at Fairchild, it was obvious that a fast fix had been made by CSI with no attention to details. A stud had been adapted to the existing high voltage stud to give the correct thread and length and a ring of aluminum had been bolted to the existing ground ring through the holes which already existed to give the correct ground ring height. The bolts were countersunk too deeply into this extension ring and there was severe nonuniformity of what should have been an exceptionally flat surface in the four bolt locations. It was obvious that an attempt had been made by CSI to correct this defect by filling the depressions above the heads of the bolts with soft solder, but this only made the areas more bumpy. In order to decrease the width of the ground ring to the specified value, the ground rings were turned down on a lathe. In doing this, the bolts placed to hold the extended portion of the ground ring in place were actually cut through and the threads could actually be seen when the ring was viewed

TABLE 2. CAPACITOR TEST DATA

Capacitor No.	Capacitance $\pm 1\%$ (μf)	Weight (kg)	Resistance ($\text{m}\Omega$)	Inductance (nH)	Energy Density (J/lb) at 2740V
1	49.43	1.878	7.9	40.1	44.8
2	49.43	1.878	9.6	42.6	44.8
3	49.70	1.880	7.7	42.3	45.0
4	49.76	1.886	5.2	39.5	44.9
5	49.64	1.879	5.2	39.6	44.9
6	46.15	1.899	6.2	42.9	41.4

from the side. Four new holes spaced 90° were drilled and tapped into the new ground ring assembly to yield the correct thread and concentricity.

Although Fairchild Republic was not satisfied with the modifications that CSI incorporated, the program was already behind schedule due to the necessity of having the terminal geometry reworked and it was decided to go ahead with the capacitors in the condition received. The units all measured 3.25 inches (8.26 cm) in diameter by 6.75 inches (17.12 cm) long. Construction consists of a single capacitor winding with extended foil terminations at each end. Other pertinent data are presented in Table 2. The resistance and inductance of each unit were obtained by shock excitation through inductive coupling of a sharp voltage spike into the capacitor and observing the resultant ring-out on an oscilloscope. Note that the energy density rating is based on 2740V. At 2500V (the original specification assuming 60 microfarad units), the capacitors are still above 40 J/lb with the exception of unit #6 (34.3 J/lb).

In order to provide a redundant seal around the capacitor terminals the entire volume between the ground ring and positive stud was potted by Fairchild Republic with Epon 828 semirigid epoxy. A bead of this epoxy was also formed around the seam between the cylindrical can and back lid as well as over the filler hole plug. After curing, the units were vacuum soaked for 48 hours at room temperature and 10^{-5} mm Hg. Inspection afterwards showed that five out of the six capacitors had leaked oil from the areas around the sides of the ground ring where the threads referred to above were visible. The entire area around the ground ring of each unit was therefore also potted in an attempt at sealing those leaks. Another vacuum soak at room temperature indicated no further visible leaks and it was assumed that the units were sealed at that time. Capacitor problems which arose during testing of the thruster system are discussed in a subsequent section of this report.

5. PROPELLANT FEED SYSTEM

a. Storage Geometry

The required total impulse of 37,500 lb-s (155,875Ns) generated at a specific impulse of 1500s requires a propellant weight of $37,500/1500 = 25$ lbs (11.36kg). The total volume of solid Teflon propellant corresponding to this amount is $25/.078 = 320.5$ in³ = 5,252 cm³ (the specific gravity of virgin TFE is $2.16 = .078$ lb/in³). The cross-sectional area of either of the two propellant rods fed into the sides of the thruster nozzle is 3.9 in² (25.16 cm²). Thus, if each rod were a straight rectangular section, the length of each section would be $1/2$ of $(320.5/3.9) = 41.09$ in = 1.044m.

This geometrical configuration would of course be impractical since it would result in an overall lateral dimension of 6.85 ft to accommodate propellant storage.

The second storage configuration considered was two semicircular sections each having the required length. The mean radius of each section would then be $41.09/\pi = 13.08$ in (33.22 cm). This implies an overall thruster diameter of 27.46 in (69.75 cm) which, although geometrically more practical than straight rods, is still considered to be too wide for practical purposes. The basis for consideration of a circular rod stems from testing done at Republic on a 20J engine in which over 21 inches of propellant were fed successfully [2] using a circular rod having rectangular cross-section.

The next most logical extension of the circular geometry is a helical coil of propellant. Based on known dimensions of the power converter and capacitors an inside radius of 7.35 inches (18.67 cm) appeared to be the lower limit if all electronic components were to be contained within the helix. Thus, the outside diameter would be 17.32 in (0.44m) which is more in line with a practical size unit. The mean radius of the helix is 8.0 in (20.32 cm). Hence, each propellant rod would have to turn through $(41.09/8.0) (180/\pi) = 294.3$ degrees. The pitch of the helix is governed by the height of the propellant rods (3.0 in = 7.62 cm) plus .25 in (6.35 mm) for support structure between the rods where they pass over one another.

The basic thruster geometry which evolved as a result of these preliminary considerations is shown in Figure 4. The total volume needed to enclose the entire propulsion system is $2356 \text{ in}^3 = 1.36 \text{ ft}^3 (.0386\text{m}^3)$, which is well below the 1.5 ft^3 contractually imposed as an upper limit.

Experience gained in the first phase of this program led to the conclusion that there was a significantly different propellant burning rate along the length of the electrodes. This conclusion was reached once it was observed that two rods of propellant which started out being perfectly parallel to one another in the nozzle area would, after several thousand discharges, become divergent. As a result of this change in the gap geometry an associated drop in thrust/power and increase in specific impulse at constant efficiency was observed. These results were in accordance with work done previously [4] at Republic wherein the angle between the propellant rods was purposely varied parametrically to determine the effect of various electrode/propellant geometries on performance. Since a constant performance level is desired for obvious

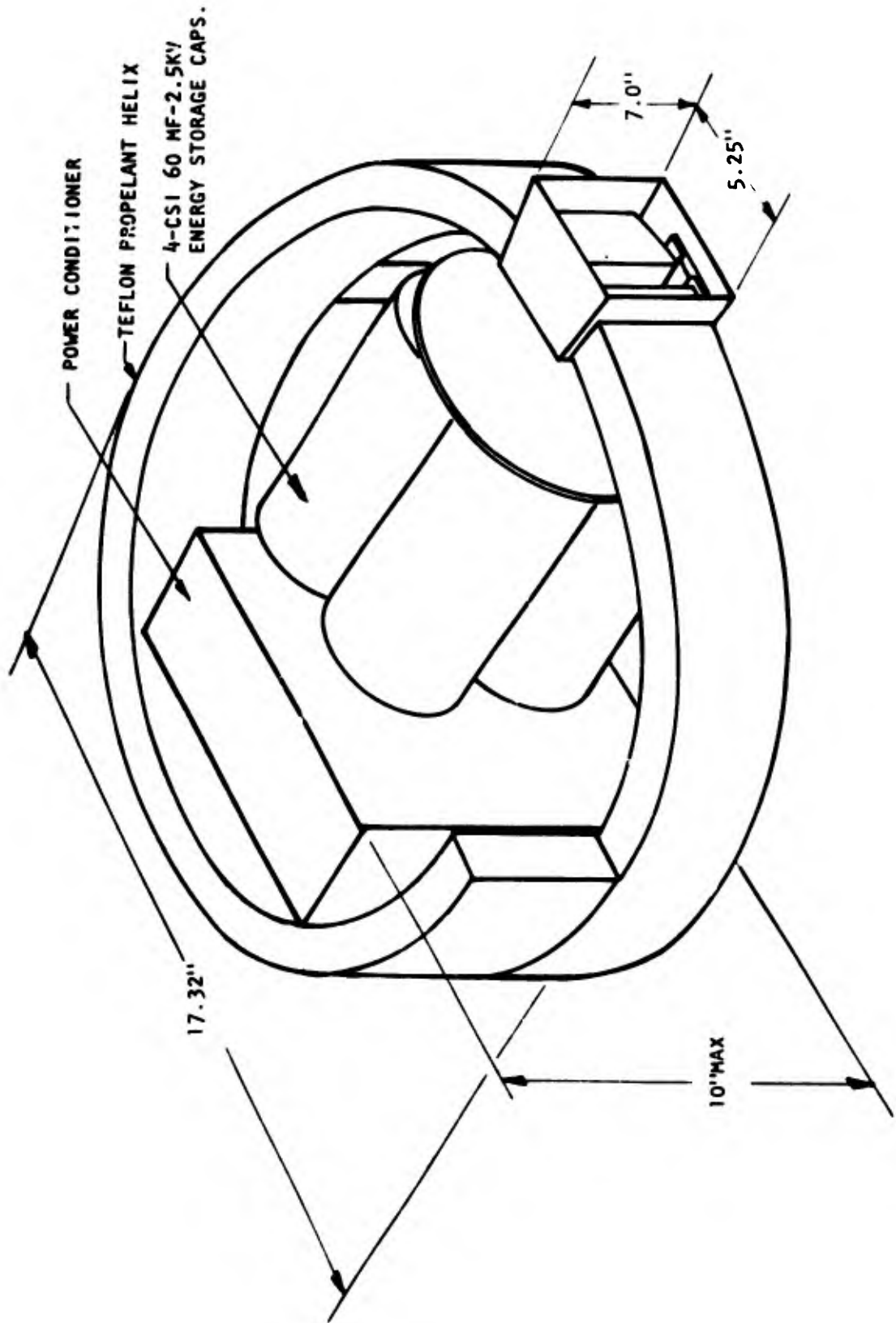


Figure 4. Basic Thruster Configuration

reasons, the change in propellant geometry could not be tolerated. A solution to this problem was to divide each of the two side fed propellant rods into several sections along its width and to feed each separate section independently. A variation in the burning rate from section to section could then be accommodated for by simply increasing the length of the faster burning sections and decreasing the length of the slower ones while keeping the total weight of propellant constant at 25 lbs. Without having any previous experience of feeding the side-fed configuration it was not possible at the onset of this program to predict the various lengths of each propellant section or even how many separate sections would be required. Procurement of the Teflon had to be initiated early, however, since machining the helix would be a long-lead item. Hence, two lots of four separate circular cylinders of Teflon were molded and then ground to fit one within the other. The thickness of each cylindrical section was 0.325 in (8.26 mm). The smallest cylinder had an inside diameter of 14.70 in (37.34 cm) and the largest had an outside diameter of 16.30 in (41.40 cm). The overall height of each cylinder was 6.5 in (16.5 cm), which gave enough material to produce two helical sections 3.0 in (7.62 cm) high having a pitch of 3.25 in (8.26 cm) and an overall mean length of 51.2 in (1.3m) based on an 8 in mean diameter and complete 360° arc. A mean diameter of 15.975 in (.502m) for the outermost section would allow for a difference in burning rates between it and the innermost section of about 25%, which appeared to be a good upper limit at the time the material was procured.

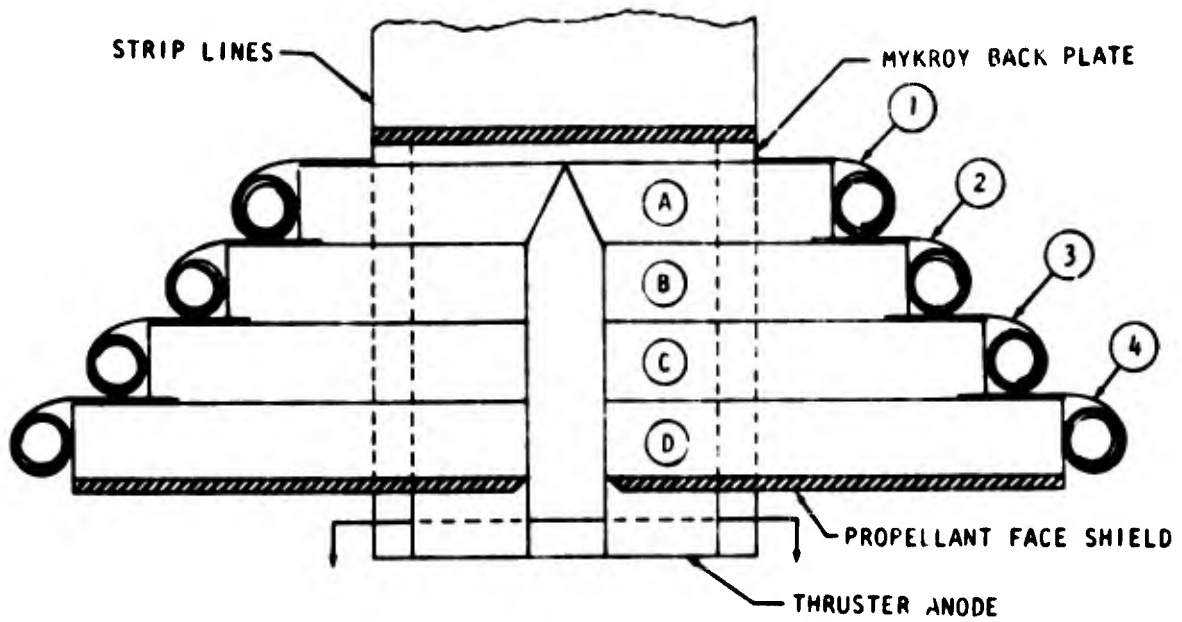
b. Preliminary Propellant Feed Tests

Before proceeding with the detailed design of the thruster nozzle and associated electrodes and insulation components a series of preliminary tests were made using the Maxwell Mylar capacitor bank fabricated for testing during the first phase of this program. The side-fed geometry with four separate straight sections of rectangular Teflon stock, each having a thickness of 0.324 in (8.26 mm), being fed from either side of the interelectrode gap was tested. The purpose of this series of tests was threefold:

- (i) To determine what specific locations in the nozzle area were potential problem spots wherein carbon deposits would build up and possibly cause a high resistance short to develop between the anode and cathode:

- (ii) To determine exactly the relative burning rates of each Teflon section so that this data could be used to calculate the length to which each section of the helical rods would have to be cut;
- (iii) To find out what other problems might arise as a result of thermal expansions of the electrodes, insulation materials, and the Teflon propellant itself.

One of the first questions which had to be resolved was how to feed the individual propellant sections independently. Normally, when a single propellant rod is used, a negator spring is fastened at one end close to the entrance to the interelectrode gap and the other end of the coiled spring is fastened at the back end of the propellant rod. When the negator spring is extended in this way, a constant force is placed on the rod which pushes it into the interelectrode gap. A small shoulder, machined into the anode surface, retains the rod in the correct position at the entrance of the gap. This same technique could be employed to feed the innermost straight rod section but the other three sections could not be fed in this manner since there would be no point close to the interelectrode gap to which the other end of each spring could be secured. The idea of using spring loaded motors to pull cables which could be fastened to the ends of the rods was investigated briefly, but this idea was abandoned due to the excessive weight of such a feed system (there would be six spring motors required) and insufficient space in the electrode region to mount all of the spring motors. After an evaluation of several approaches the feed system finally adopted was as follows. The innermost propellant section would be fed in the usual way; i. e., a negator spring fastened at a point close to the entrance of the interelectrode gap and at the rear of the propellant section. On the basis of our previous experience it was clear that each succeeding section would have to be longer than its predecessor since the burning rate would be increasing from the back strap out to the exit plane of the thruster nozzle. Thus, a spring fastened at the rear of the innermost section and to the back end of the adjacent Teflon section (which is longer) would be extended and would cause the adjacent section to feed independently so long as the first spring had sufficient force to overcome its own friction and the force of the second spring. If the same principle is applied to the next two sections of propellant, it is found that the governing force is that required to overcome static frictional forces on the outermost section. This principle is depicted below in Figure 5.



TOP VIEW-CATHODE OMITTED FOR CLARITY



ANODE CROSS-SECTION

Figure 5. Schematic of Propellant Feed System Used for Preliminary Testing with Straight Rods

Individual propellant sections A, B, C and D are fed by springs 1, 2, 3, and 4, respectively. The propellant sections are held in position by the retaining shoulder machined into the anode. Note that rod A is Vee-shaped and that the fuel retaining shoulder in the anode has a corresponding shape. This is done to relieve the heat load on the

Mykroy insulator at the back strap once the arc is initiated. Mykroy is used to shield the face of rod D which would have a tendency to burn away due to the heat energy radiated to it from the expanding plasma plume. Experimentation with the hardware revealed that a force of three pounds (13.35N) was necessary to overcome frictional forces on rod D. The force exerted by Spring A was therefore 3 lbs. In order that spring 3 be capable of feeding rod C a force of 3 lbs plus an additional 5 lbs to overcome frictional loads on C was necessary. Thus, spring 3 produced 8 lbs (35.4N). Following the same arguments, spring 2 exerted a force of 12 lbs (53.4N) to feed rod B and spring 1 produced 19 lbs (74.55N) to feed rod A. These forces were actually provided using a number of springs having the same output and size because of space limitations.

c. Results of Preliminary Testing

A photograph of the nozzle showing the straight propellant rods is presented in Figure 6.

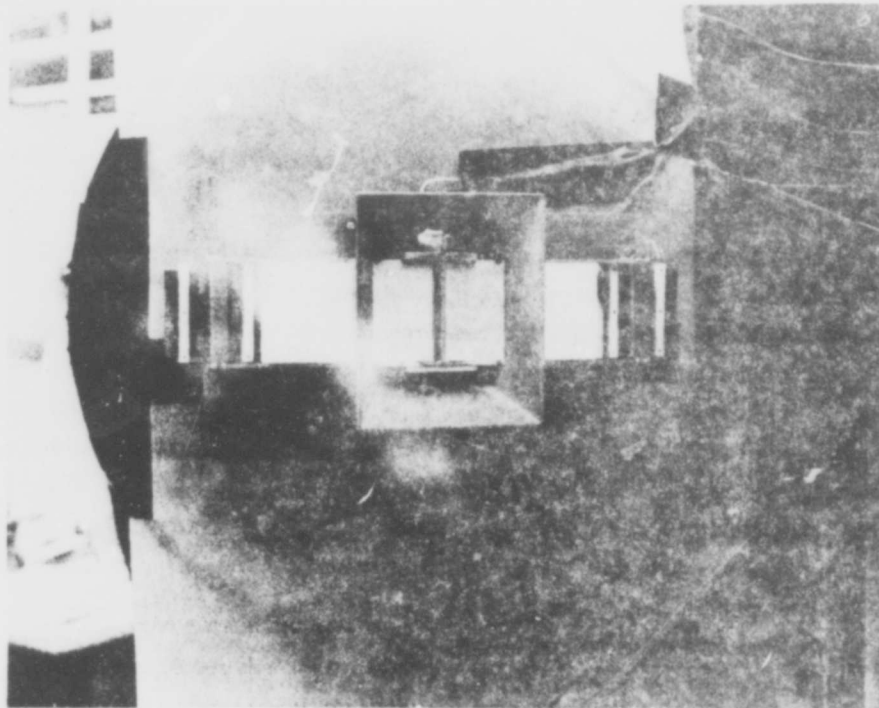


Figure 6. Prototype Nozzle Using Straight Propellant Rods

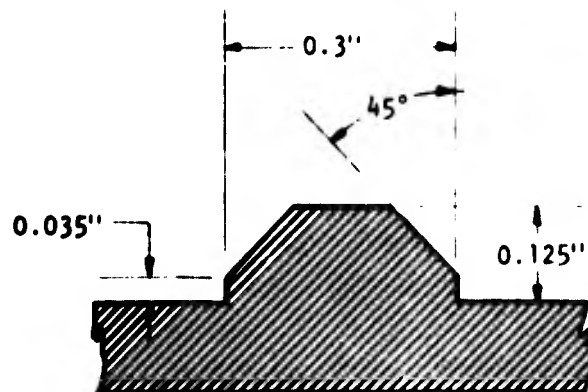
Initial testing identified several problem areas. The first of these indicated two critical locations within the arc volume wherein carbon deposits caused high resistance shorting between the thruster anode and cathode. These shorts developed after only a few thousand discharges. One of these locations was along the Mykroy insulating back plate. The innermost propellant rods had a tendency to burn slightly nonuniformly along their height and this caused a diverging gap to develop from anode to cathode. The area in this gap left the Mykroy directly exposed to the arc and carbon tended to build up on this surface resulting eventually in a short. This problem was remedied by slotting the Mykroy across its width and grinding down the side of the slot facing the arc. The carbon build up on the back plate is completely isolated from the cathode by the slot and gap. The only way in which a short could develop would be if the entire slot filled up with carbon. The slot is sufficiently deep to prevent this from occurring.

The other area which caused electrical shorting resulted from there being a tendency for carbon to deposit on the top surface of the propellant (cathode side) and along the edge of each separate rod. This deposit caused tracking from the cathode, along the surface of the Mykroy insulation around the sides of the cathode, across the top surface of the propellant and down the edge of the rod to the anode. This condition was corrected by interrupting this path with another slot located between the propellant guide track and cathode.

Having solved the tracking problems it was possible to begin evaluating the propellant feed system over large numbers of thruster discharges. During one test approximately 10,000 discharges had been accumulated when it was observed that the propellant rods had apparently stopped feeding. Several tests were run to determine why this was occurring. The problem was finally diagnosed as being a result of thermal expansion of the Teflon propellant rods in the longitudinal direction which was causing them to bind against one another after sufficient firing time elapsed to produce a high enough propellant temperature. Once the ultimate temperature of the confined portion of the propellant rods was determined (approximately 350° F) the required amount of clearance was calculated to be .02 inches (.508 mm). Results of previous tests, however, showed that if any clearance existed between the separate sections of propellant this would lead to an expansion of the arc into this clearance which would further increase the size of this clearance and eventually cause a catastrophic failure because of the pressure which would build up, force the sections apart, and result in structural damage to the supporting guide. Hence, in order to allow for the thermal expansion the

Mykroy propellant face shields had to be spring-loaded. This would allow the propellant to expand while maintaining enough force between the sections to keep them in contact during the expansion, yet not enough force to cause them to bind due to friction.

Incorporating the spring loaded face shields allowed accumulation of considerably more discharges before another problem was encountered. The shoulder height used was based on that which has been used on breech-fed microthrusters produced in the past. This height is .055 in. (1.4 mm). In the nozzle configuration of the present program it appeared that the same shoulder height was too large to allow sublimation of the Teflon area in contact with it. As a result, the propellant was burning at a faster average rate above the shoulder than below and this caused the spacing between propellant rods to increase across the major portion of their height above the shoulder. It was clear, therefore, that if thruster performance was to be maintained the shoulder height would have to be decreased so that the spacing between propellant rods could be held. The question that immediately arose was how much to decrease the height by. Not having any idea as to what the appropriate height should be the existing shoulder was taken down in .01 in (0.25 mm) stages and testing continued. A shoulder height of .035 in (.89 mm) appeared to be acceptable, although the propellant spacing was still somewhat larger than the desired value. It was decided not to decrease the shoulder height any more than this since the bearing pressure on the propellant rods has an upper limit before plastic deformation becomes a problem. Moreover, since the shoulder actually forms the surface of the anode as far as the arc is concerned, erosion of the shoulder had to be considered. It was obvious to the naked eye that the erosion rate, if it continued to be as severe as was observed would eventually eat away the entire shoulder at the center. To eliminate this possibility a new design of the shoulder was incorporated. The shoulder cross-section was changed from rectangular to polyhedron in the shape shown below:



With the above geometry the propellant bearing surface (i.e., the two vertical sides) and sublimation rate are maintained at the value found acceptable through experimentation while the shoulder height at the center provides enough material to offset the effects of electrode erosion.

Using the new shoulder geometry improved the maintenance of propellant spacing considerably. Testing was carried out for roughly 13,000 discharges when another problem arose. The area of Teflon in proximity to the ignitor plug appeared to be ablating faster than any other area surrounding the arc. As a result of this erosion an indentation was formed in this area. Unfortunately, the interface between the innermost and adjacent sections of propellant rod was situated in the center of this indentation and the arc was finding its way between the two sections because of this. Eventually, the pressure which built up between rods A and B during a discharge forced the entire assembly to fail structurally. It was evident that an interface at this location was not going to work. To confirm our hypothesis of this failure mode sections A and B of the propellant rods were replaced by a single propellant section having a thickness of 0.650 in. (1.65 cm). The Vee shape for the first half of this new rod and the parallel wall geometry for the remaining half were retained so that all other geometric considerations were identical. A test was then initiated and ran until all available propellant was consumed. A total of 120,000 discharges were achieved without interruption. For the first time the side fed electrode/propellant geometry had been successfully fed for a significant length of time (over 240 hours).

With this successful run the design details of the electrode/propellant configuration were frozen. Only one condition had to be rectified - - the Teflon cylinders procured for fabrication of the helix and which were in the process of being machined were procured with the intention of having four individual sections rather than three. Inquiries concerning cementing the two innermost sections together were immediately made and, fortunately, it was found that there was a special cementing process which could be used to give a reliable bond.

The data resulting from the above test yielded the following relative amounts of Teflon ablated from each pair of propellant sections:

- (i) Innermost Sections (Exposed Area = $3.90 \text{ in}^2 = 25.2 \text{ cm}^2$) = .3356
- (ii) Next Sections (Exposed Area = $1.95 \text{ in}^2 = 12.6 \text{ cm}^2$) = .3012
- (iii) Outermost Sections (Exposed Area = $1.95 \text{ in}^2 = 12.6 \text{ cm}^2$) = .3632

The total mass ablated was $203.3682\text{g} = .4485\text{ lbs}$. On a per unit surface area basis the amounts of mass ablated were 37.88 g/in^2 (5.87g/cm^2), 31.41g/in^2 (4.87g/cm^2), and 17.50g/in^2 (2.71g/cm^2) for the outermost, middle, and innermost sections, respectively. This confirmed the original postulate that the mass ablation per unit area increases along the length of the electrodes. Using the above data the total length of each section of helical propellant rod was calculated. For the innermost rod a total of .3365 times 25 lbs, or 8.39 lbs (3.805kg) of propellant would be required. The cross-sectional area is 1.95 in^2 (12.58 cm^2) and the mean radius is 7.675 in (19.495 cm). Hence, the length of each half of the innermost section is $4.195\text{ lbs}/(.078\text{ lbs/in}^3 \times 1.95\text{ in}^2) = 27.58\text{ in} = .70\text{m}$. This length would therefore require a subtended arc of 206 degrees for each half of the innermost helical section. Following the same logic, the middle propellant section would be 7.53 lbs (4.415kg) at a mean radius of 8.162 in (20.73 cm) and each half-section would subtend an arc of 347.5 degrees. The outermost section would be 9.08 lbs (4.118kg) at a mean radius of 8.487 in (21.55 cm) with each half-section subtending 403 degrees. The required arc length of the outermost section posed a new problem since the cylindrical Teflon sections which were procured and were in the process of being machined to the helical shape were only high enough to generate a maximum 344° of usable helix. The length of time necessary to procure cylinders of sufficient height to refabricate the middle and outermost sections was prohibitive from a program scheduling standpoint. A reverse calculation was performed assuming a 344° subtended arc for the outermost half-section and working backwards to determine the total propellant weight on that basis. The weight of each outermost half-section would be $(344/403) \times 4.54\text{ lbs} = 3.875\text{ lbs}$ (1.758 kg) yielding a total propellant weight of 7.75 lbs (3.515 kg) in the outermost helical sections. Dividing this by the relative consumption rate obtained experimentally give the total propellant weight storable. Hence, $7.75/.3632 = 21.34\text{ lbs}$ (9.68 kg). This represents a 3.66 lb (1.66 kg) overall decrease of propellant which results in a decrease in total impulse capability from 37,500 lb-s to 31,860 lb-s (141,713Ns).

An evaluation of the above dilemma led to the decision to proceed with design and fabrication of the thruster with existing resources and accept the reduction in total impulse capability. The situation would not have existed had experimental data concerning relative consumption rates between propellant sections been generated prior to procurement of the materials necessary to fabricate the helical rods. Since it was

not possible to obtain such data a priori and still have enough time to procure the Teflon within the overall time-frame of this program, the predicament could not be avoided. Moreover, a deficit of 5640 lb-s (28,087Ns) only represents 15% of the total requirement and essentially no redesign of the thruster structure or components would be required to produce the total impulse called for if the additional propellant were made available at a later date. It was also reasoned that to provide laboratory data on the capability of subsystems the thruster could be refueled after 31,860 lb-s was generated with enough additional propellant to produce the entire required life.

Proceeding with the design on the basis of 344° outermost half-sections it is found that the intermediate half-sections each weigh 3.214 lbs (1.458 kg) and subtend 296.4° and the innermost half-sections each weigh 3.581 (1.624 kg) and subtend 175.8°.

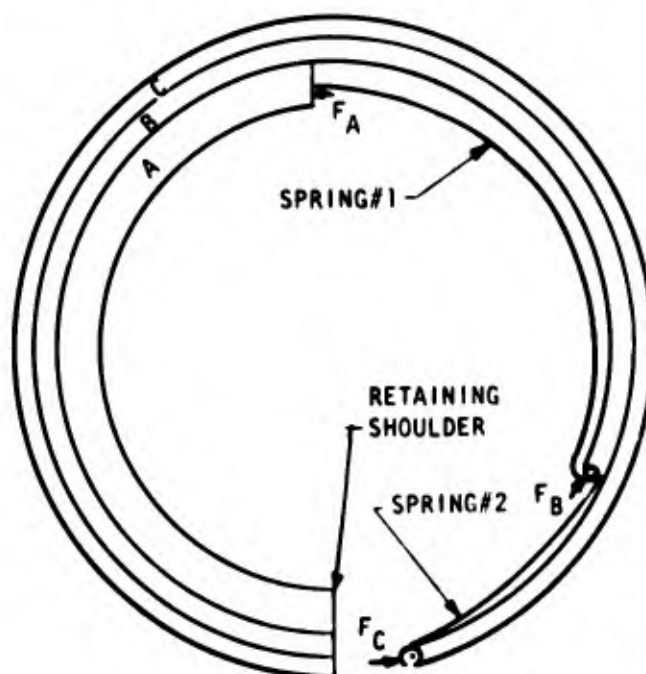
After delivery of the fabricated helical propellant rods the two innermost sections of each rod were cemented together. To insure a uniform pressure over the large surface area (to which the cement was applied after etching) the rods were clamped and then placed inside a collapsible bag which was evacuated. This insured a uniform pressure equal to atmospheric pressure over the entire area. The three sections of each rod were then cut to their appropriate lengths and the innermost sections were machined to the Vee-shape as shown in Figure 5.

d. Propellant Support Structure and Helical Feed System

The helical propellant rods are supported by a series of 13 aluminum brackets fastened to a continuous ring cut from .125" (3.08 mm) phenolic. To insure smoothness of operation and minimize friction the location of each support bracket was determined by calculating the coordinates of the helix at each bracket location and using a height gauge to pinpoint the position of each. Then, after assuring perpendicularity, the brackets were fastened in place.

The feed system adopted for preliminary testing using straight propellant rods was incorporated. This involved fabrication of spring-driven B-motors (constant output torque) to pull cables fastened to the innermost helical sections. The use of a cable rather than a negator spring was necessitated due to space limitations in the immediate vicinity of the electrodes and current collecting stripline. The B-motors could be mounted in a more spacious area and the cable directed via pulleys. The

other two helical sections were fed using negators in the manner described previously. After assembly of the thruster system each section of the rods was tested for free movement by displacing it from its position at the retaining shoulder and observing whether or not it sprung back into position. This was found not to be the case. It was observed that the sections would move freely when the cable pulling the innermost section was released. To understand why this occurred refer to the diagram below. In addition to the forces shown there are frictional forces between the sections (at the interfaces between A and B and C.) The magnitude of these frictional forces is in direct proportion to the magnitude of the forces pushing the sections into the retaining shoulder. Since movement of the sections is microscopic during normal feeding the



situation can be considered static. Force F_A is applied to section A by the cable. Spring #1 pulls section B from the back and also exerts an equal force on section A since it is fastened to the back of section A. This force on section A opposes F_A so F_A must be greater than F_B . Similarly, F_B must be greater than the force exerted on section C by spring #2. Determination of the magnitude of the required forces F_A , F_B and F_C was done experimentally by first measuring the force necessary to overcome static friction on section C. Forces F_B and F_C were then scaled up accordingly. When the entire system was loaded, however, it was immediately obvious that these forces were not large enough. The reason it appeared that more force was necessary

stems from the fact that pulling the propellant sections from the back was effectively pushing them outward and together, causing them to bind due to friction at their interfaces. Moreover, the more force one applied to section A so that it would feed, the more the tendency for B and C to bind (since the pressure at the interfaces increased) and the larger F_B and F_C had to be. Experimentation with various combinations of forces did not lead to a solution and, eventually, it became apparent that this feed system could not be implemented with reasonably sized forces. It is important to note that no such problem existed when straight propellant rods were fed because there was no interrelationship between the retarding frictional forces and the magnitude of the force pushing each section. It is the helical geometry that causes this interrelationship and the same condition would exist if purely circular sections were used.

The above approach to independently feed the helical sections was abandoned and new ideas were generated and evaluated. During this period some preliminary performance and thermal-vacuum testing was carried out with the thruster system and propellant using an interim solution of the feed problem. This interim solution involved using a separate spring to feed the outermost section. This spring was run around the outside of that section with the take-up spool mounted near the entrance to the thruster nozzle. A spring with roughly 6 lbs (26.7N) force was required. This approach eliminated the need for spring #2 in the above diagram and allowed section B to move freely with 6 lbs of force exerted by spring #1. It was concluded that feeding section A from the back end would not work because of the resulting load produced on the interfaces between sections. The interim solution consisted of extending a spring between the two innermost half-sections of propellant and attaching the spring at each end to take-up spools fastened to the half-sections at points close to the nozzle entrance. About one-sixth of the total propellant could be fed in this manner and preliminary tests were initiated to generate data on thruster performance and thermal conditions. These initial tests also allowed for verification of allowed thermal expansion clearances. Results of those tests are discussed in a subsequent section of this report.

The method finally arrived at for feeding the innermost sections of propellant consisted of pulling the sections into the retaining shoulder from the back while physically constraining the sections around their outside circumference so that there would be no load imparted to the two outer half-sections. Thus, the helix is essentially

split by a .040" (1.02 mm) thick aluminum rail which separates the inner and two outer half-sections on each side and absorbs the outward load exerted by the spring feeding the innermost rod. The rail does not separate the propellant sections over the entire circumference since they must all eventually come together at the nozzle entrance, but the distance over which this occurs is small enough to keep the frictional loading at an accepted level. A photograph of the thruster showing the splitter rail is presented in Figure 7.

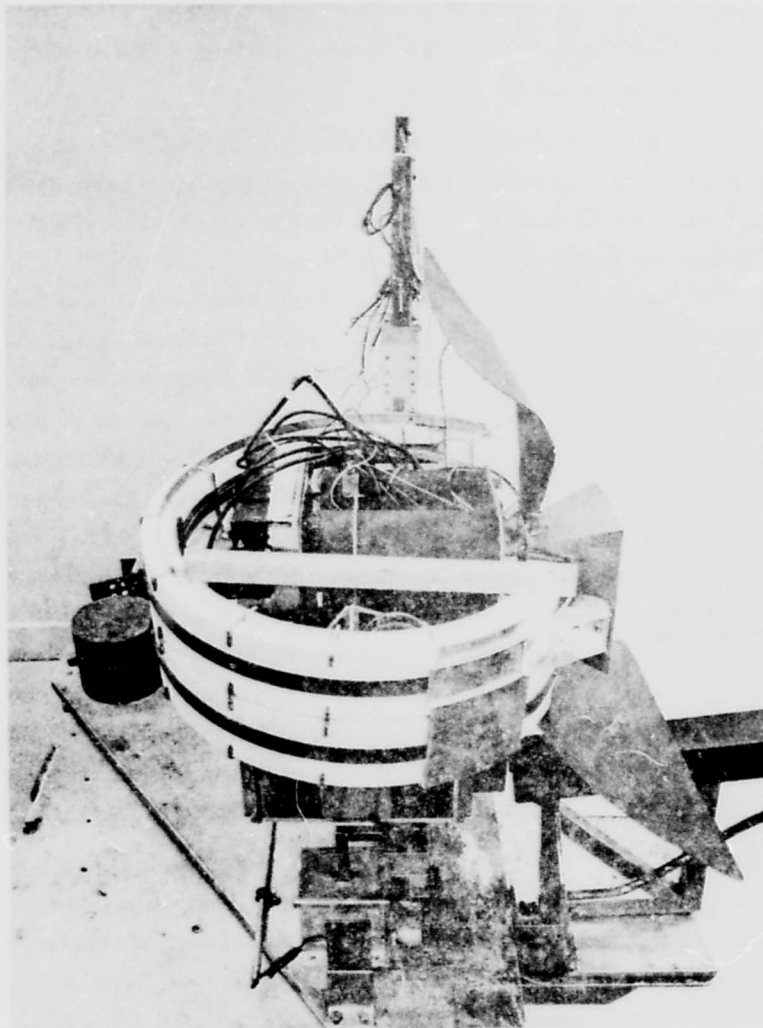


Figure 7. One Millipound Thruster System With Helical Solid Propellant Storage

III. RESULTS OF THERMAL-VACUUM AND PERFORMANCE TESTS

1. THERMAL-VACUUM TESTS

Testing was carried out to determine the long-term thermal characteristics of the thruster system in a vacuum. The maximum allowable equilibrium temperatures of the various thruster subsystems are well defined. The KF-film thruster capacitors should not reach temperatures exceeding 45°C because of the severe decrease in life expectancy beyond this point. The upper limit on the temperature of the power converter was set at 60°C, and the basic result of allowing circuit elements to exceed this temperature is a decrease in the conversion efficiency. Initial testing was done with the power converter outside the vacuum chamber.

Iron/Constantine thermocouples were placed in five locations on the thruster immediately behind the anode and the cathode of the thruster nozzle, and on the ground ring, side, and back lid of one of the KF-film capacitors. Normally, the capacitor dissipation factor is low enough and the size of the capacitor large enough to obtain thermal compatibility through thermal radiation by means of the capacitor external surfaces alone, assuming the power level per capacitor is not excessively high. A Mylar capacitor having the same size and weight as the KF-film units used on this thruster would not normally overheat at the power input per capacitor being used (i.e., $111/4 = 27.75\text{W}$) if the power loss through its own internal dissipation were the only source of heat. Previous experience, however, has shown that there is another significant potential external heat source for the capacitors associated with pulsed plasma thrusters: namely, heat generated at the thruster nozzle anode and cathode. This heat is due to the continual surface bombardment of high energy particles which carry the arc current. The resultant heat loading on the electrodes has been observed to be as much as ten to fifteen percent of the total input power [5]. Since an excellent path for conduction of electrical current between the capacitors and electrodes is built into the thruster, the heat generated at the electrodes will conduct just as readily back to the capacitors if it is not intercepted by a parallel path and conducted elsewhere.

Questions arising because of the relatively high dissipation factor associated with KF-film and the uncertainty regarding the actual amount of heat being conducted back to the capacitors from the electrodes prompted the need for a test to get an

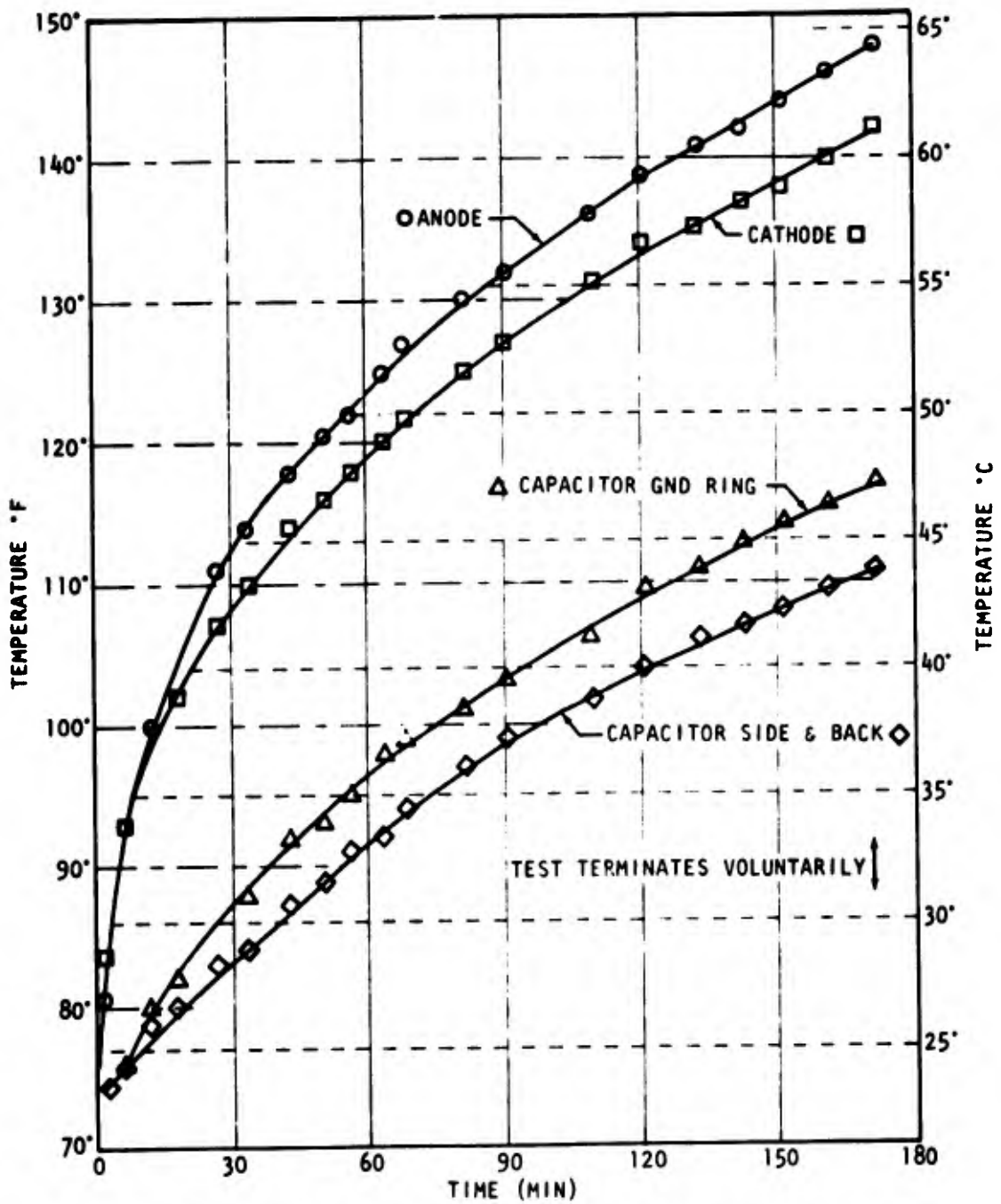


FIGURE 8. TEMPERATURE VS. TIME AT VARIOUS LOCATIONS ON THRUSTER

engineering estimate of the amount of heat which had to be dissipated to keep the capacitor temperature below the 45°C upper limit. The data obtained from this test are plotted in Figure 8. The results are as expected with the temperature decreasing as the distance from the electrodes increases. One noteworthy fact is that the side wall and back lid of the capacitor remained at the same temperature throughout the test. This result was encouraging since there was some speculation before running the test as to whether or not the end terminations of the foils at the back of the capacitor can had sufficient cross-sectional area to carry the current (about 23,000A per capacitor at peak current) without building up severe current densities which would tend to heat the back end of the capacitor. This test showed that the construction technique used by CSI in terminating the foils and the design of the collection tabs themselves was adequate for this application.

The thermal gradient between ground ring and side of the capacitor indicates that heat was indeed conducted from the electrodes, across the strip line, and into the capacitors. The rate of increase of temperature with time at the electrodes and at the ground ring asymptotes approximately the same value of .01°F/s. Based on this rate, the estimated heat generated at the electrodes is about 15W or 13.6% of the total input power. Intercepting this flow of heat and conducting it to roughly 1460 cm² of radiator area* at 40°C radiating to the walls of the vacuum chamber (24°C) would be sufficient to keep this 15W away from the capacitors, assuming of course that the conduction path to the radiators is at least as good as the path directly through the copper strip lines. The radiators, however, would have to be insulated from the electrodes and this dictated the need for an electrically insulating, thermally conducting material which could be used to interface between electrodes and radiators. Beryllium Oxide is such a material, having a thermal conductivity roughly equivalent to Aluminum while its properties as an electrical insulator are excellent. Slabs of BeO .125" (3.3mm) thick, large enough to cover the area of the back strap portion of the electrode, i. e., 1.5" (3.71cm) x 2.25" (5.72cm), were available with a solderable metal film on both faces. These slabs were soldered to the anode and cathode. A copper adapter plate, to which the radiators were bolted, was soldered to the other face of each BeO slab. Thermally conducting grease was used at the interface between the copper adapter plate and radiators to assure good thermal contact. The radiators were fabricated from Aluminum plate and painted black to yield good emissivity.

* All thermal testing was carried out without providing a conduction path between the thruster and the thruster mounting hardware. In an actual spacecraft application conduction cooling to the spacecraft structure via the mounting hardware is generally permissible. Therefore, the thermal tests performed are more severe than probably ever would be encountered in an application. Indeed, the radiators incorporated would probably never be required in practice.

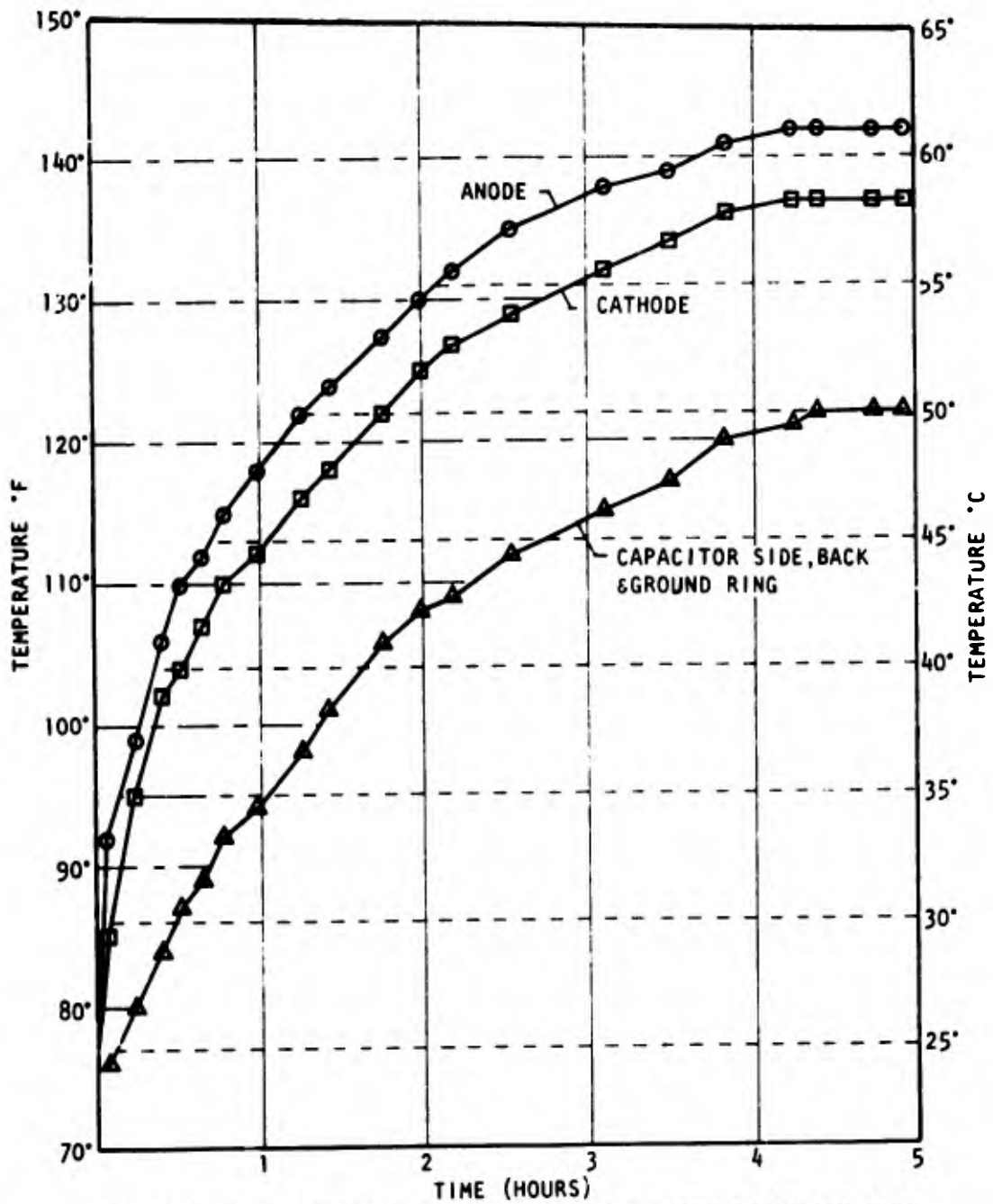


FIGURE 9. TEMPERATURE VS. TIME INCLUDING ADDED RADIATION AREA

Thruster testing continued after installation of the radiators. Thermal data taken with the radiators are presented in Figure 9. Thermal equilibrium was attained after about 5 hours of continuous operation. The capacitor ground ring temperature at that time was 50°C, 5° higher than the "maximum allowable" value. Testing was not discontinued at 45°C, however, because no temperature gradient existed between the ground ring and side of the capacitor can with the radiators installed. It was reasoned, therefore, that the radiators were efficiently intercepting heat generated at the electrodes and that the capacitors were heating up for the most part as a result of their own internal dissipation. The close similarity between the thermal data at the back and sides of the capacitor can both with and without the radiators also supports this supposition. The test was continued in order to allow a determination of the ultimate equilibrium temperature of the capacitors with the only mechanism for heat removal being radiation from their own surface area. Knowing this, it would be possible to estimate the amount of heat which had to be removed by conduction directly from the capacitors to additional radiation area. The effective radiation area of the four capacitors, in the configuration which they are mounted, is equal to the surface area of a single cylinder having the same outside diameter as one of the capacitors plus four times the area of the back lid. This effective area is approximately 102 in² (658cm²). A perfect black body having this surface area would radiate 11.58W at 50°C to a 24°C enclosure. This estimate appears to be on the high side, that is, it seems unlikely that this amount of power (roughly 10% of the total power input) is being dissipated by the capacitors, especially when it is realized that the dissipation factor of KF-film at 50°C and 10⁵Hz has a maximum value of about .04 [6], implying a maximum of only 4.4W of dielectric losses. There are of course other loss mechanisms within the capacitor (in particular, resistive losses along the discharge path) which could account for the additional 7W of calculated power loss but it is more likely that the assumption of perfect black body radiators and/or the estimate of the effective radiation area are incorrect to some degree. Nevertheless, a value of 11.5W serves as an upper limit on the amount of additional heat to be disposed of in order to reduce the capacitor temperature from 50°C to 45°C by radiation only. Conducting this amount of heat from the back lids of the capacitors using BeO discs and routing the heat to additional radiation area would be the simplest way to dispose of it. A calculation shows that 680cm² more radiation area would be required for disposal of the 11.5W at 40°C

to the 24°C enclosure. The thruster was not modified to include the additional radiation area because the power converter first had to be integrated for determination of the total thruster heat load in its final geometry. These calculations are based upon the constraint of utilizing radiation cooling without conduction cooling through the thruster mounts.

Resolution of other problems encountered later on in the program did not allow additional thermal-vacuum tests with the total integrated system so no additional thermal-vacuum data was obtained.

2. THRUSTER PERFORMANCE

In addition to thermal-vacuum testing, a test was performed to verify the performance level of the thruster, excluding the power converter. It was believed that such a test should be performed prior to putting the thruster system on life-test because of uncertainty concerning the higher dissipation factor associated with KF-film as compared to Mylar. The performance demonstrated during the first phase of this program was generated on a laboratory test thruster using twelve 9 microfarad Mylar capacitors placed in parallel. Not only was there some question concerning the energy delivery efficiency of the new KF-film units but another unknown had been introduced by changing the magnitude of capacitance used to store the 750J. The original laboratory thruster consisted of about 109 microfarads charged to 3710VDC and the prototype millipound thruster uses 200 microfarads charged to 2740VDC. What effect changing the combination of capacitance and voltage to deliver a given energy has on thruster performance is one aspect which has not been investigated in detail at Republic. Although no evidence exists which demonstrates any significant change in performance as a result of varying capacitance and voltage at constant energy, there was some limited semi-empirical work done in the first phase of this program that suggests the invariance of performance with respect to capacitance and/or voltage as independent variables.

A total of 2506 thruster discharges were accumulated during the performance test with a total of $3.7924 \pm .002g$ of propellant ablated. The mass-per-discharge of propellant was therefore 1.5133mg or 3.3368 micropounds. The impulse bit was measured every 500 discharges. The measured impulse bits varied between 5.909 and 6.121 mlb-s with a test average of 5.987 mlb-s (26.63 mNs). Hence, the specific impulse is $(5.987/3.3368) \times 10^3 = 1794s$. This is about 19.6% higher than the program

goal of 1500s. The capacitance used was 198.2 microfarads and the voltage 2740VDC giving an energy of 744J. The thrust/power ratio is then $5.987/744 = 8.05\text{mlb/kW} = 35.80\text{mN/kW}$, or 10.6% lower than that required to obtain one millipound with 111W of power at the capacitors. The thrust efficiency ($T^2/2mP$) is 31.5%.

Although these results show that both efficiency and specific impulse exceed the individual program goals, the thrust/power level is not sufficiently high to generate the required 1 mlb thrust level with the maximum input power called for. In order to generate one millipound of thrust, 124.2W would be required at the capacitors or 154.5W at the input to the power converter (at 80.4% conversion efficiency). At 2500 VDC the power requirement would be reduced to 152.6W at the converter. It is important to note that the 1 mlb thrust level can readily be obtained at the 1794s and 31.5% efficiency level by simply increasing the thruster pulse frequency from 0.148Hz to 0.166Hz.

The decrease in thrust/power and corresponding increase in specific impulse when compared to the values obtained during first phase testing are attributed to the difference in spacing between propellant rods encountered as a result of feeding the rods and allowing them to reach their equilibrium ablation contour. During first phase testing the demonstration of performance was done without feeding the rods and generally no more than 1000 discharges were accumulated in any one performance test. The rods used during this performance test had experienced a total of 8900 discharges at completion. It is believed that the performance data quoted above is probably the "long term" level (i.e., after burn-in) because of the relative constancy of the impulse bit over the entire 2500 discharges. As mentioned in a previous section of this report, the burning rate at the retaining shoulder appears to be slightly slower than over the exposed propellant surface. This leads to a widening of the gap between propellant rods and causes less mass to be ablated per discharge leading to a decrease in thrust/power and compensating increase in specific impulse and efficiency. This tendency toward a wider gap between propellant rods is clearly illustrated in Figure 10, which is a photograph of the thruster nozzle taken after the performance test was completed.

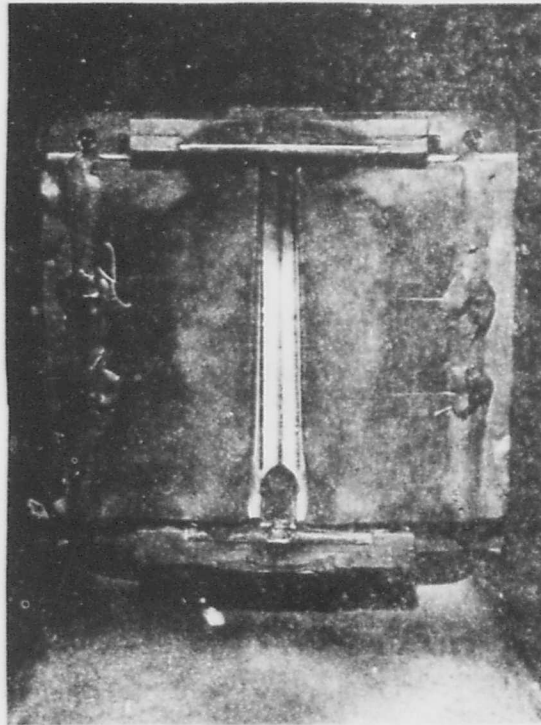


Figure 10. Thruster Nozzle After Performance Testing

The net effect of these changes in performance parameters, aside from leading to a higher power requirement, will increase the total impulse capability with a given amount of propellant and also increase the total required life of the capacitors. At 1794s the 21.34 lbs (9.68 kg) of propellant could yield 38,284 lb-s (170,287Ns) of total impulse, thereby surpassing the required 37,500 lb-s. Indeed, at this new specific impulse the required propellant weight for 37,500 lb-sec would be reduced to 20.90 lbs (9.48 kg). The capacitor life expectancy for generation of 37,500 lb-s would be increased since the impulse bit is smaller than expected. The required life is 6.264 million discharges (or, roughly 700,000 more discharges) which represents an increase of 12.7%. To consume the available propellant (38,284 lb-s) a life of 6.395 million discharges would be necessary.

On the basis of the above results a summary of the program objectives and actual capability is presented in Table 3.

**TABLE 3. SUMMARY OF PROGRAM OBJECTIVES
AND ACTUAL CAPABILITY**

Program Objective		Actual Capability System
Specific Impulse	1500s	1794s
Thrust Efficiency	30%	31.5%
Overall System Efficiency	24.36% min. (26.7% goal)	25.33% (25.6% at 2500 VDC)
Thrust at 137W Input	1 mlb	0.894 mlb
Required Power for 1 mlb Thrust	137W max.	154.5W (152.6W at 2500 VDC)
Total Impulse Capability	37,500 lb - s	37,500 lb - s (38,284 possible)
Volume	1.5 ft³	1.36 ft³
Weight	45 lb	50.23 lb (22.79kg)

IV. PERFORMANCE OF THRUSTER SYSTEM

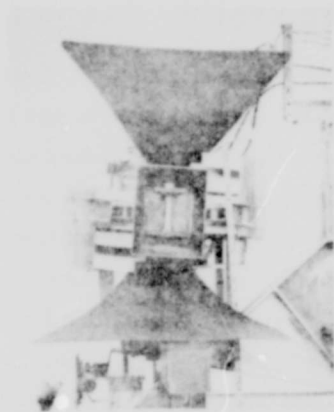
Having resolved all functional problems encountered it was possible to put the thruster on life test. Photographs of the thruster system are presented in Figure 11. The thruster was mounted on a thrust balance so that thrust could be monitored continually throughout the test. Other instrumentation included thermocouples to monitor temperature and a 1000 : 1 Tektronix voltage probe to monitor high-voltage output from the power converter. Power was supplied by a 28VDC source and the SCR triggering pulse input to the discharge initiating circuit was provided from a signal generator, both of which were outside the vacuum chamber. Means for measuring input current and voltage to the power converter were also provided so that the conversion efficiency could be periodically checked.

The first attempt at firing the thruster with the integrated power converter resulted in an electrical breakdown between the high voltage output lead and discharge circuit ground. This occurred because the leads were routed too close to the circuit board at the point of attachment to the capacitor collector plates. The converter would not operate properly after this incident and had to be sent back to Wilmore Electronics for repair. Thruster testing began, however, using power supplies to provide the 2740VDC and 620VDC. These were to be replaced by the power converter once it was repaired.

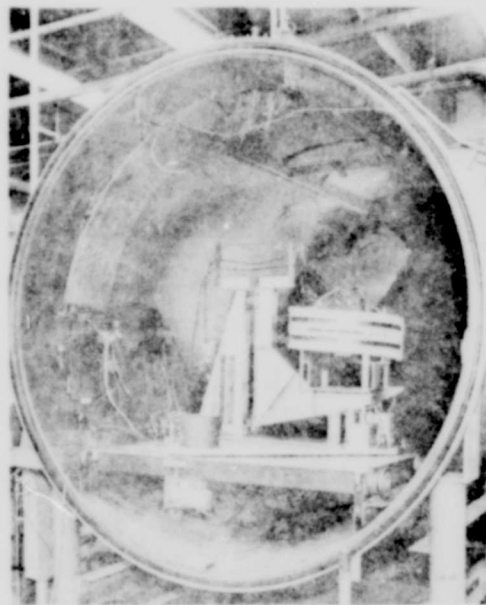
A system weight breakdown is presented in the following table.

<u>Component</u>	<u>Weight</u>	
	<u>Pounds</u>	<u>kg</u>
Discharge Module		
Electrodes, Collector Plates & Ignitor Plug Assy.	2.121	0.962
Discharge Initiation Circuit	0.838	0.380
Mykroy Back Plate & Face Shields	0.353	0.160
Exhaust Cone	<u>0.765</u>	<u>0.347</u>
Sub Total	4.077	1.849
Capacitors (4)		
	<u>16.571</u>	<u>7.515</u>
Sub Total	20.648	9.364
Power Converter	<u>4.750</u>	<u>2.154</u>
Sub Total	25.398	11.518
Main Support Structure	1.625	0.737
Radiators	.823	.373
Feed Spring Assemblies	<u>1.863</u>	<u>0.845</u>
Sub Total	29.709	13.473
Propellant	<u>21.340</u>	<u>9.685</u>
Total Weight	51.049	23.158

The design weight of 45lbs was exceeded by only 11%.



(a) Front View



(b) Thruster on Thrust Balance in Vacuum Chamber

Figure 11. Photographs of Thruster System

After initiating testing one of the CSI capacitors failed after 5338 discharges. This capacitor had accumulated only 14,769 discharges at 2740V at the time of failure. Subsequent examination revealed a hole in the side of the capacitor can towards the terminal end (see Figure 12).

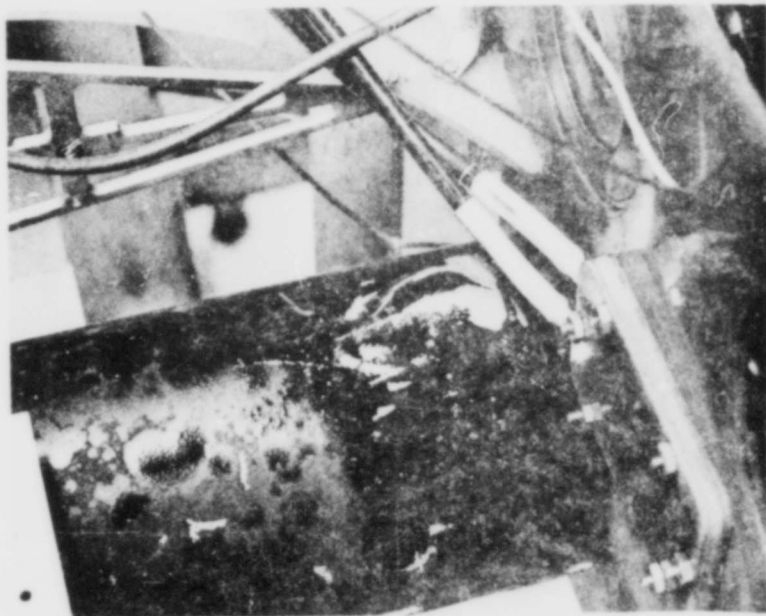


Figure 12 . Capacitor Failure

The location of this failure, i. e. , at the top of the can when viewed with its axis of symmetry positioned horizontally suggests that the cause of failure was an air bubble in the oil impregnant which eventually rose to the top of the can. The presence of a void in this location generally results in a flash-over from the high voltage terminations (or the closest foil) to the capacitor case, which is at ground potential. Since this capacitor was one which had leaked during the original vacuum soak it is likely that a void was present in the impregnant.

The failed capacitor was replaced with a spare unit after the thruster had been disassembled to clean off all oil residue. Testing was resumed and 3114 discharges later a severe drop in the thrust level was recorded. The test was stopped and the chamber opened to determine the reason for this. It was immediately obvious that

another CSI capacitor had failed. This failure caused structural damage to the collector plate assembly and associated electrical insulation. The damage was extensive, and caused the positive collector plate to completely detach itself from the positive stud on the failed capacitor. Thus, the capacitor failure did not appear as a short (as was the case when the first unit failed) since it was effectively taken out of the circuit (see Figure 13). The physical shape of the capacitor had been distorted by the failure. Both ends of the can were noticeably bulged outward. A measurement of

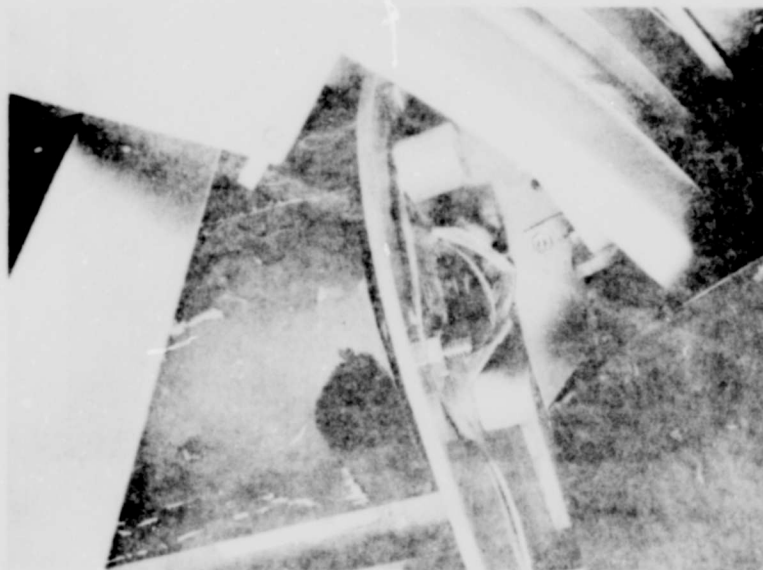


Figure 13. Second Capacitor Failure

the capacitance on an impedance bridge showed that the unit was not shorted and still indicated the correct value of capacitance. The dissipation factor, however, was much higher than the value originally measured on this unit. Characteristically, this kind of failure is exhibited when a collection tab on either end of the winding separates or burns out. It is not believed that the loss of oil impregnant could result in this kind of failure but this may indeed be the case.

The strip line assembly was refabricated and the last spare capacitor was placed on the thruster. By the time these rebuilding efforts were completed the power converter, having been repaired, was also integrated with the output leads

now routed properly. Wilmore found a shorted inductor in one of the input EMI filters to be the only element damaged by the previously cited electrical breakdown. Thus, the entire thruster system was again placed in the vacuum chamber for testing.

It was not possible to generate any more significant life on the propulsion system from that time on. Capacitors continued to leak and cause breakdowns. These leaks were apparently microscopic in size since visual evidence of oil did not exist when the units were examined. All leakage was in the area around the positive stud and ground ring. Various tests to determine the exact location of the leaks were unsuccessful. Stripping existing potting and repotting the leaky units was not successful either. Eventually, it was decided that everything that could possibly be done by Republic to insure a leak tight capacitor had been carried out. All of the normal procedures which have been successful in sealing commercially available capacitors were performed on the CSI units and it still appeared that no guarantees could be made concerning the seal. Aside from dictating to the manufacturer what procedures are necessary to insure a hermetic seal, and instituting the proper quality control and assurance at each step in the fabrication of the capacitors prior to their delivery, there was nothing which could be done at Republic to seal off the units in our possession.

Efforts during the remainder of the program (approximately one month) were therefore concentrated on the design and fabrication of the propellant feed system components required to feed the entire length of the propellant sections. It was felt that this approach would make available, at program completion, a system requiring only a reliable bank of capacitors for immediate life test. Complete redesign, fabrication, and assembly of the feed system was accomplished and the system was checked for smooth operation with the full compliment of propellant rods. The check was a success and the capability to reliably feed the entire available propellant exists.

V. RESULTS OF RFI TESTING

1. GENERAL

Measurements of the radiated radio frequencies emitted by the arc discharge during thruster firing were made. Characterization of the RF energy emanating from the thruster is important because of the potential interference with satellite communication and control systems which could result during thruster operation. Other potential sources of interference are conducted electromagnetic energy and induced voltages generated by the time varying arc voltage and current.

Previous studies by Dr. K. Thomassen (7) have shown that pulsed plasma thrusters emit a pulse of RF energy at the instant the arc is initiated and that this pulse is virtually the only source of noise throughout the thruster discharge. Thomassen's measurements were made using horns and spiral antennas. Measurements were broadband with a 16J thruster source.

Aerospace Report No. TOR-1001(2037)-4, Reissue B, dated 15 August 1972 was used as a guide for all measurements which were made. A test plan, based on this document when applicable, was submitted to AFRL and approved prior to initiating tests.

Data taken during the program being reported upon provides the following information:

- (i) The amplitude versus frequency spectrum of the radiated Poynting flux per unit bandwidth (S_{ν})
- (ii) The effect of initial capacitor voltage and energy on S_{ν}
- (iii) Broadband measurements of Poynting flux per unit bandwidth
- (iv) The effect of exhaust cone scattering of RF energy at $8 \pm .050\text{GHz}$

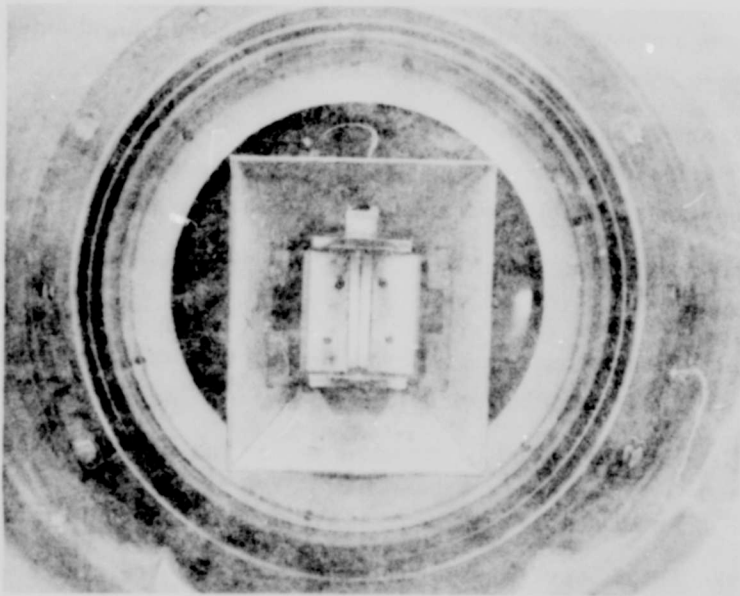
Conductive EMI measurements were not made because due to capacitor problems the entire thruster system could not be operated for any significant length of time.

2. EXPERIMENTAL SET-UP AND EQUIPMENT

The RF measurements were made with a thruster situated in a 6' x 8' vacuum chamber. The thruster nozzle protruded through a window in the chamber wall to which a glass tube 1' in diameter by 3' in length was attached. Photographs of the set-up are presented in Figure 14. The glass tube was used to reduce the effects of electromagnetic scattering and the fittings and collars are all made of nonmetallic materials.



(a) Vacuum Chamber with 3 Foot Glass Extension Tube



(b) View of Nozzle Looking Into Glass Extension Tube

Figure 14. RF Measurement Set-Up.

Measurements were made with broadband detection systems. Figures 15 and 16 show the combinations of components used to make these measurements.

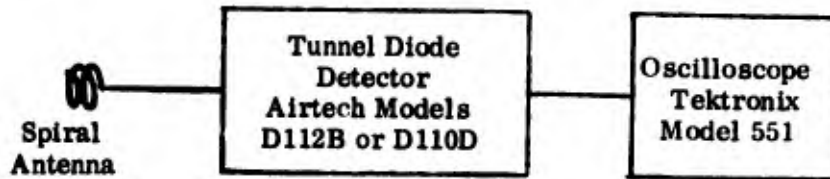


Figure 15. Broadband Detection System

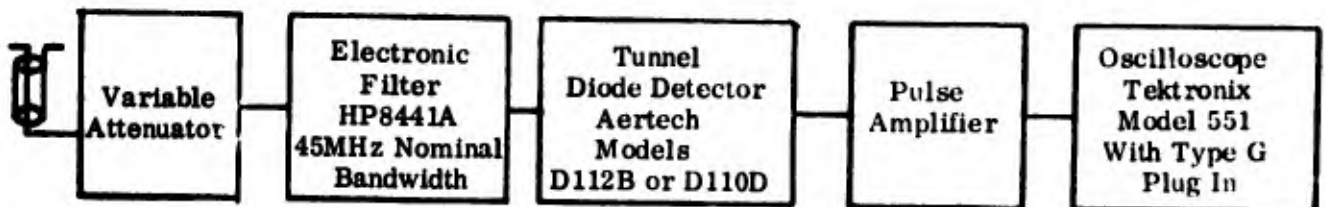


Figure 16. Broadband Detection System Used For Narrow Band Measurements

The video bandwidth of the detection system is approximately 24MHz, and the rise time is 16ns (governed by the oscilloscope whose rise time is 15ns with the plug-in amplifiers used). The fastest thruster RF pulse which was recorded is shown in Figure 17. The rise time is 20 to 30ns. The pulse width was seen to be variable and is generally between 100 and 300ns when observed with the detection system shown in Figure 16.

The pulse amplifier in Figure 16 consists of an RF amplifier and an amplifier to drive a 50 ohm cable. The 3 db bandwidth of the amplifier is 70MHz. Figure 18 shows a block diagram of the amplifier. The gain characteristic of the amplifier is shown in Figure 19.

The video bandwidth of the tunnel diode detector is at least 100MHz. The RF antennas which were used for the measurements are tabulated in Table 4.

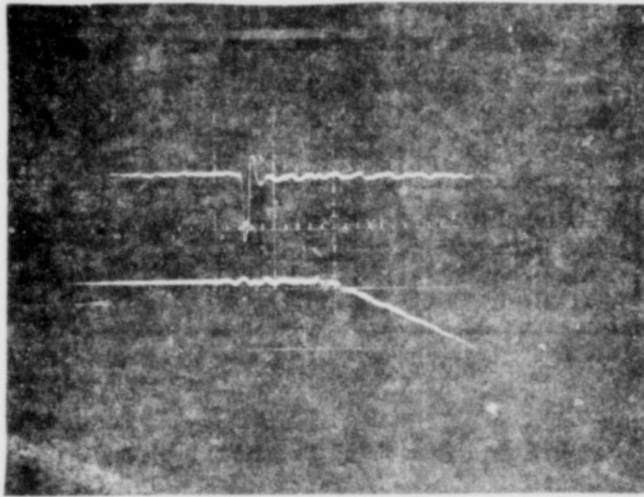


Figure 17. Typical Thruster RF Pulse-Time = $.5\mu\text{s}/\text{cm}$;
 Upper Trace = RF Pulse, $.5\text{V}/\text{cm}$,
 Lower Trace = Discharge Current, $\sim 70,000\text{ A}/\text{cm}$

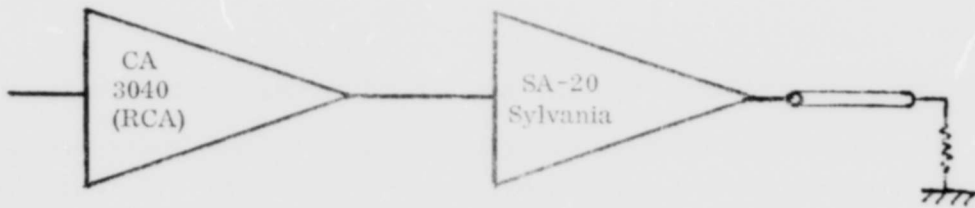


Figure 18. Schematic of Pulse Amplifier

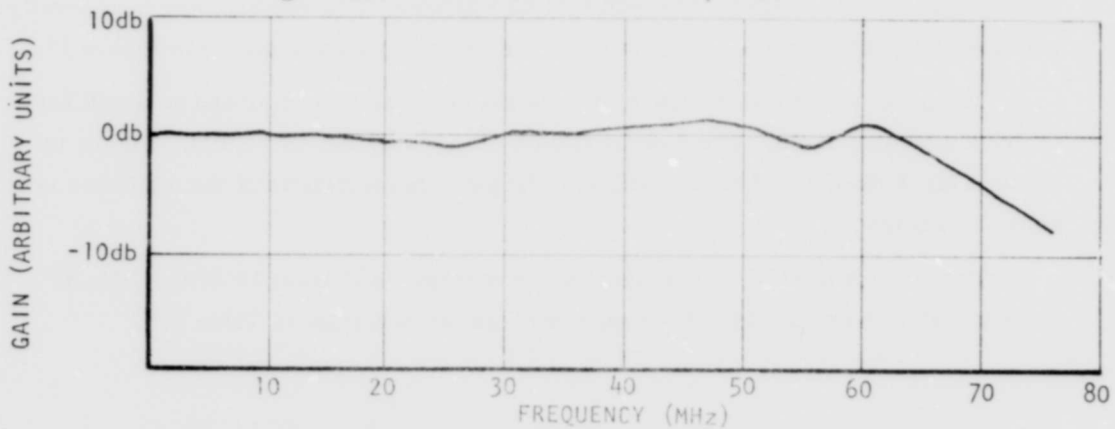


Figure 19. Gain Versus Frequency of Pulse Amplifier

TABLE 4. SUMMARY OF ANTENNAS USED FOR RF MEASUREMENTS

<u>Model Number</u>	<u>Manufacturer</u>	<u>Type</u>	<u>Frequency (GHz)</u>
DBG-520	Demornay	Standard Gain Horn 20db	8.2 -12.4
DBJ-520	Demornay	Standard Gain Horn 20db	5.85- 8.2
DBK-520	Demornay	Standard Gain Horn 20 db	3.95-5.85
DBL-520	Demornay	Standard Gain Horn 20 db	2.60-3.95
1610-18	RSI	Cavity Backed Spiral, 5db Circular	2-18
1610-12	RSI	Cavity Backed Spiral, 5db Circular	1-2
1610-05	RSI	Cavity Backed Spiral, 5db Circular	.5-1
BB-105	Empire	Broadband Discone	.020-.065
BB-105	Empire	Broadband Discone	.065-.200
BB-105	Empire	Broadband Discone	.200-.400
BB-105	Empire	Broadband Discone	.400-1.000

The detection system was calibrated by substituting a Hewlett Packard microwave generator for the antenna with the generator operating in the pulsed mode. This allowed direct calibration of that part of the detection system consisting of the pre-selector, tunnel diode detector, pulse amplifier and oscilloscope. The RF response of the tunnel diode detector was checked in a separate measurement and its response was found to be relatively flat from 1GHz to 17GHz.

Measurements were made with the thruster being operated off a 28VDC battery. This technique eliminated some of the pick-up problems originally encountered which generated noise in the detection system. Figure 20 is a schematic of the entire test set-up. All measurements were made looking directly into the thruster exhaust cone. The exhaust cone was fabricated from .125" thick Mykroy ceramic which was covered on the outside with .01" thick OFC. The copper was at thruster ground potential and was insulated from the plasma with several coats of Magna-X500 potting compound. The cone has the shape of a triangular prism with each of the four sides inclined at a 40° angle. The exit plane measures 5.8" (14.7cm) by 6.9" (17.5cm). Rectangular cutouts in two of the four sides allow the propellant to pass through the cone and into the interelectrode gap. These cutouts are 3.27" (8.3cm) high and 1.57" (4cm) wide. The overall length of the cone along the thrust axis is 3.27" (8.3cm). A drawing of the exhaust cone is presented in Figure 21.

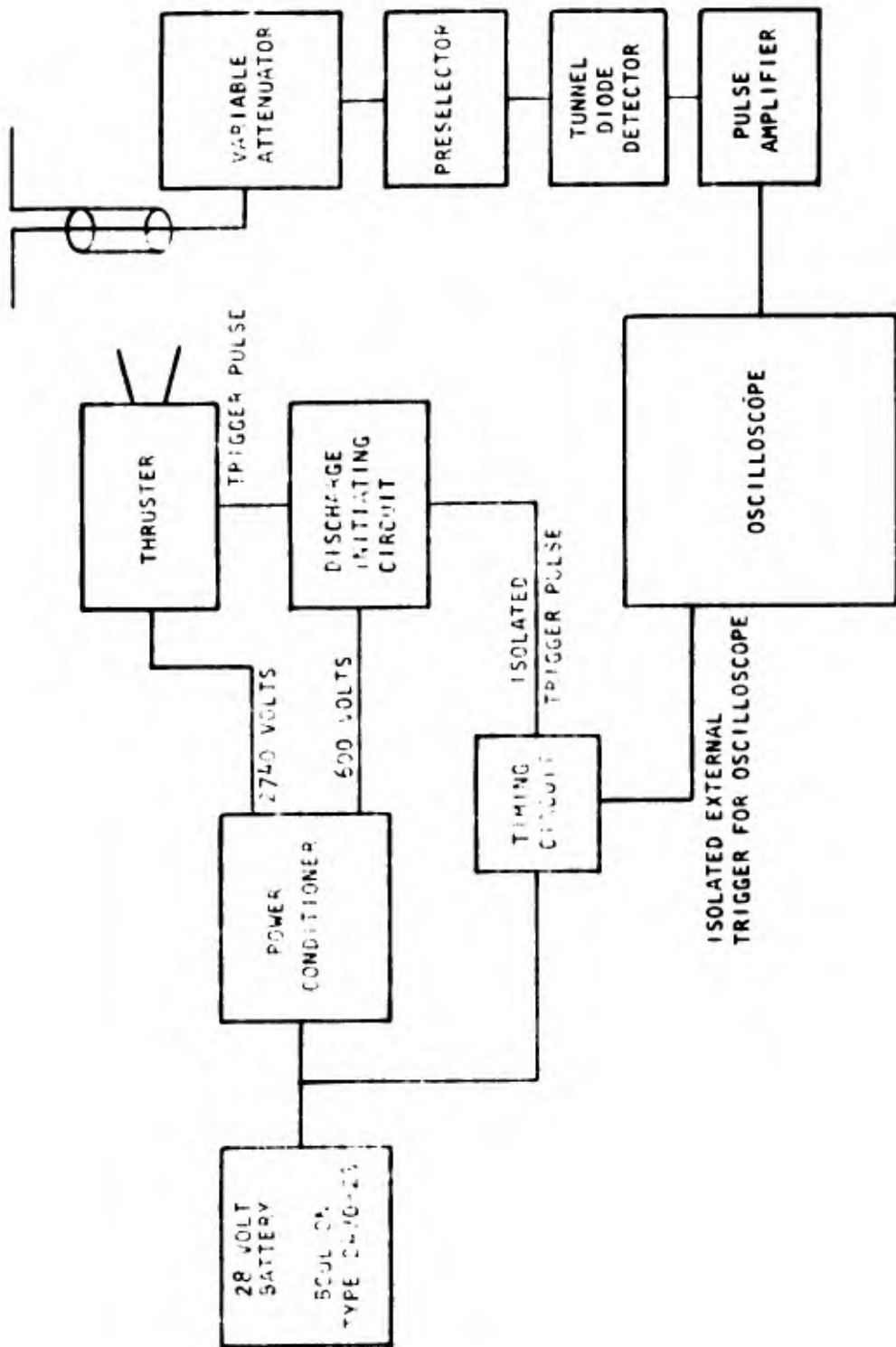


Figure 20. Schematic of Measurement Set-Up

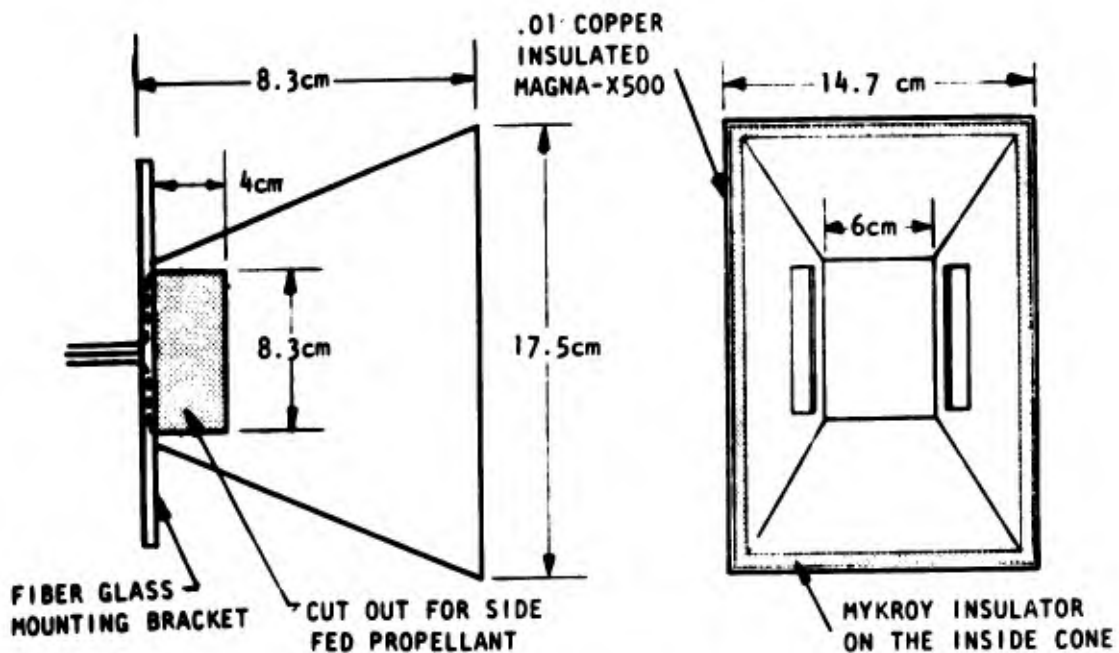


Figure 21. Exhaust Cone Geometry

3. MEASUREMENT RESULTS

a. Description of Data and Recording Technique

The magnitude of the RF spike at arc initiation was obtained through visual observation of the oscilloscope screen each time the thruster fired. It was soon found that this magnitude had a random value, i.e., changed significantly from discharge to discharge with no consistency. From an operational standpoint it was necessary to record only the maximum value of the spike over a large number of observations since it is this value which has significance with regard to interference levels. The question therefore arose as to whether or not a sufficient number of observations were being made at each detection frequency to include the maximum. Hence, a certain confidence level had to be generated to insure that the maximum spike amplitude at each detection frequency had indeed been observed. At first it appeared that 40 to 60 consecutive observations would result in recording at least one spike having the maximum value. Later it was necessary to make as many as 150 observations to obtain this maximum. From each set of readings a maximum was obtained and this value was used in the subsequent data reduction. The narrow band measurements took the longest time to record and a few frequencies were repeated to insure that the RF pulse had not changed significantly with time.

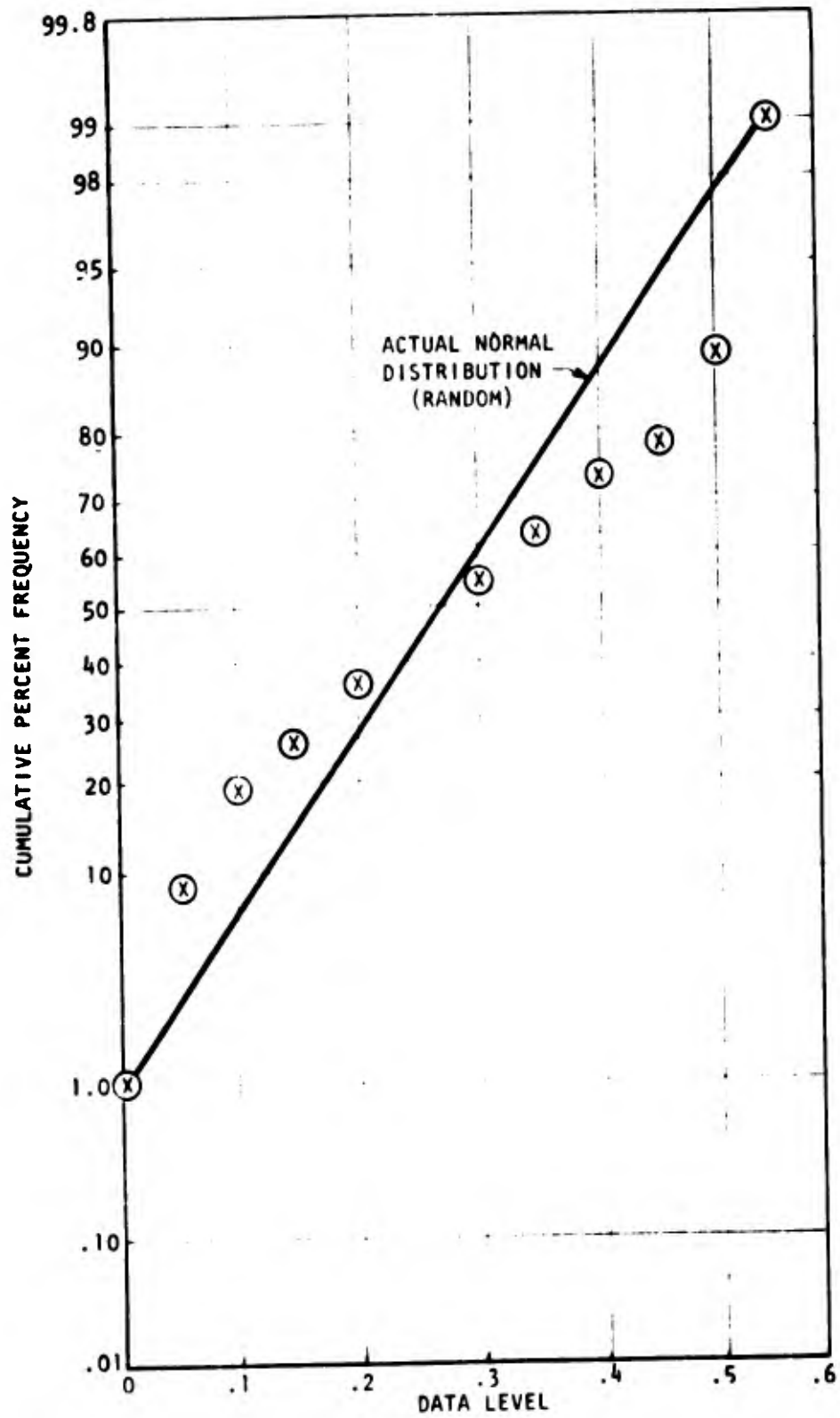


Figure 22. Cumulative Frequency Vs. RF Data Level

The distribution of the data at any detection frequency suggested that the RF pulse is a random event. To check this hypothesis a set of data was plotted on probability graph paper. Figure 22 shows this plot. The straight line indicates the curve a truly random distribution of numbers would yield. The closeness of the data to this line is a measure of its randomness [8]. For a true test many more data points would have to be included (there are 60 points represented in Figure 22) and the accuracy of the readings would have to be increased. Nevertheless, the data appears to be very nearly random.

b. RF Pattern Measurements

The scattering characteristics of the glass tube and end plate into which the thruster was fired has been checked on a previous effort at Republic. Figure 20 shows the scattering that was recorded when an X-band, 20 db standard gain horn was put into the position occupied by the exhaust cone. The measurement was made at 8GHz. The typical response of this horn in free space is superimposed on the plotted data obtained from actual measurements.

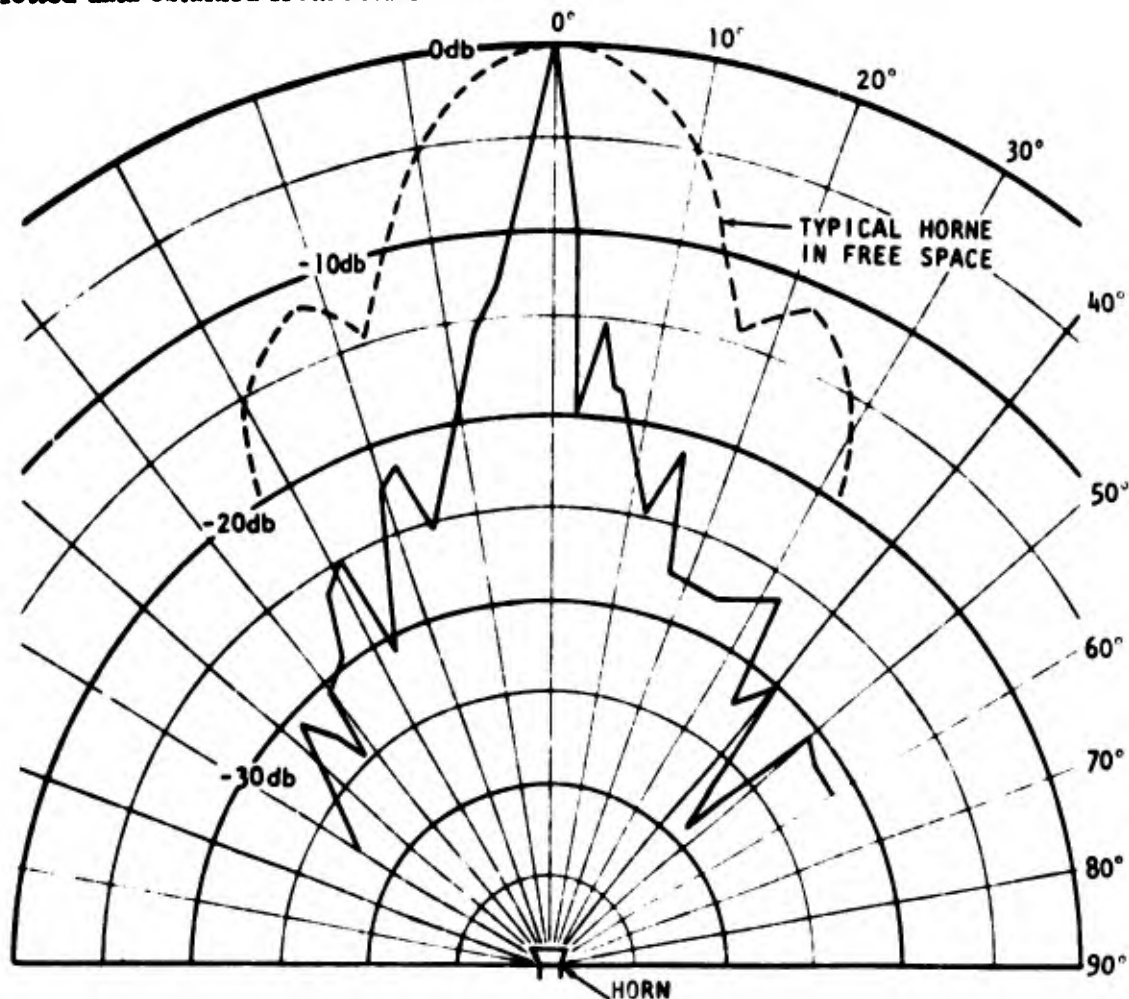


Figure 23. Pattern Measurement to Determine Scattering Effects of Glass Tube

It is apparent that the glass tube has the effect of increasing the scattering in the axial direction. Figure 24 is a schematic of the set up used to make the measurements.

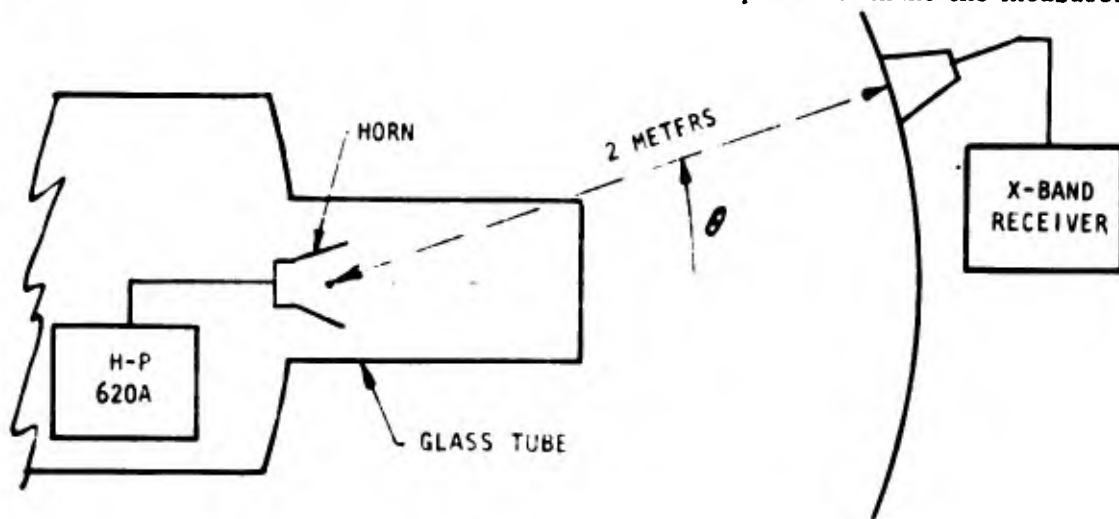


Figure 24 . Schematic of Pattern Measurement Set Up

It is believed that the scattering characteristics of the glass tube, vacuum chamber and surroundings are relatively frequency independent over the majority of the frequency range scanned.

Having determined the effect of the glass tube, a pattern measurement of the thruster exhaust was made. The measurements were made at 8GHz using the detection system shown in Figure 16. A 20 db standard gain horn was used as a receiver. The distance from the exhaust cone plane to the receiver was 2m. Several sets of data were taken at each angular position and the average is plotted in Figure 25. The maxima and minima coincide fairly well with the edge of the exhaust cone and the propellant passage plot (see Figure 21). In view of the tunneling effect of the glass tube a gain factor of 2 was assigned to the exhaust cone.

The significance of this pattern measurement is with regard to placement of antennas relative to the thruster location on a satellite. The results of this measurement show that by placing antennas outside a cone having a 40° included angle a decrease of at least 4db in the impingent RF is achieved.

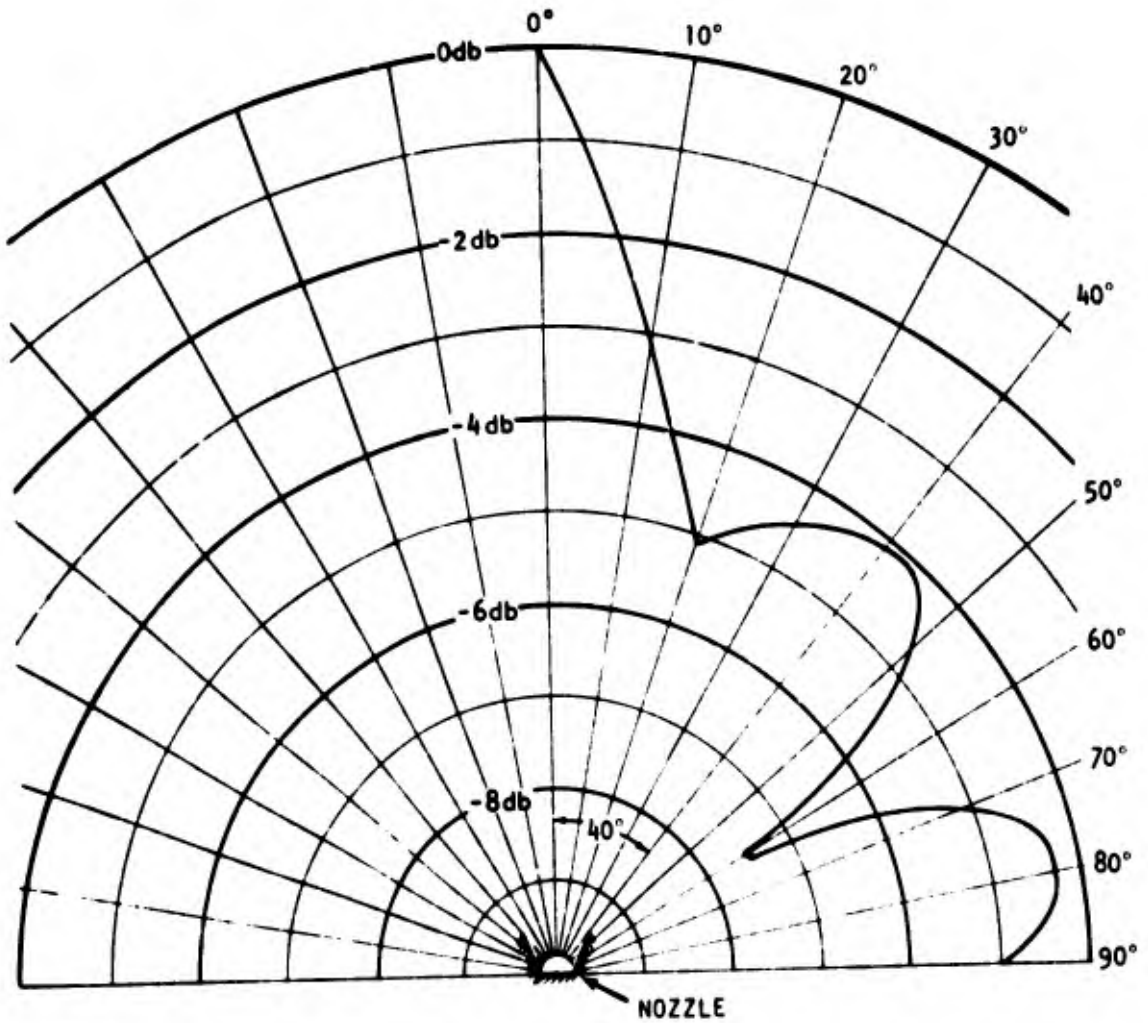


Figure 25 . Thruster RF Pattern in the H - Plane

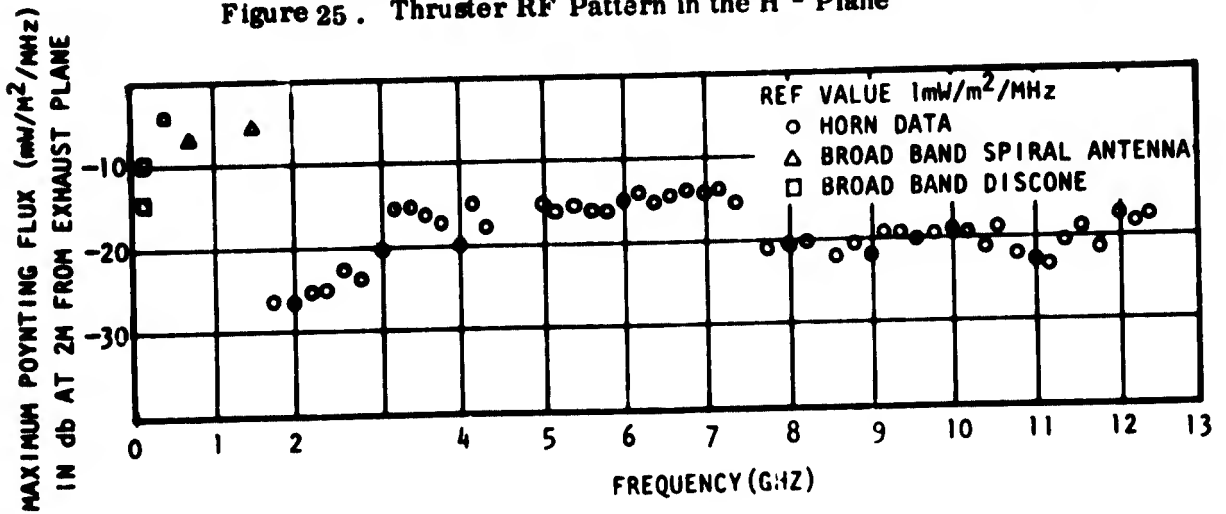


Figure 26. Frequency Spectrum of Radiated Poynting Flux

c. Data Reduction

It was indicated that the RF pulse showed great variability with respect to its amplitude on a shot-to-shot basis. Under such circumstances it seems reasonable to present only the maximum values of the pulse amplitude.

Direct calibration of the detection system allows one to relate the observed pulse amplitude to the received power, after attenuation corrections have been made. The received power is then related to the Poynting flux through the relationship

$$P_{\text{received}} = \frac{\lambda^2 G_r S}{4\pi}$$

where λ is the wavelength of the incoming radiation, G_r is the gain of the receiving antenna, and S is the Poynting flux incident on the antenna. The quantities associated with the receiving system are P_{received} and G_r . These are known quantities and S is therefore determined at the preselected wavelength. Dividing S by the RF bandwidth of the receiver yields S_ν (i.e., the flux per unit frequency), which is independent of the receiving system.

d. Narrow Band Data

The narrow band data was taken using the detection system shown in Figure 16. All of the antennas except the RSI 1610-18 were used. At the lower frequencies standard gain horns could not be used. At these points broadband antennas were used. The effective aperture value in such cases is given by

$$A = \frac{\lambda_1 \lambda_2 G}{4\pi}$$

The reduced narrow band data is presented in Figure 26. The magnitude of the Poynting flux per unit frequency is seen to be relatively constant over the major portion of the frequency range scanned. The average value at 2 meters is -18.5db corresponding to .0141 mW/m²/MHz. No attempt was made to correct the low frequency data for near field effects.

The electric field associated with the radiation flux can be calculated using the relationship

$$E = \sqrt{2\eta S_\nu \Delta\nu}$$

where E is the electric field, η is the impedance of free space (377 ohms), and $\Delta\nu$ is the receiving system band width. E is in V/m, S in W/m²/MHz and $\Delta\nu$ in MHz.

e. Broadband Data

The broadband measurements were made with a RSI 1610-18 spiral antenna (frequency range of 2GHz - 18GHz). The detector was an Aertech D112B tunnel diode having a useful frequency range of 1GHz-17GHz. This combination yields a high level signal directly displayable on the oscilloscope. The detection scheme is shown in Figure 15.

This broadband measurement was made as a check on the narrow band data. Agreement with the narrow band measurements is fairly good, with a value for S_ν of .0156mW/m²/MHz at 2m obtained as compared to the average value of .0141mW/m²/MHz resulting from narrow band measurements. No attempt was made to correct for the exact frequency response of either the detector or the antenna. It is also noted that the value quoted for the broadband measurement assumes a constant value of S_ν so that

$$P_{\text{received}} = \frac{C^2 G S_\nu}{4\pi} \left(\frac{1}{\nu_1} - \frac{1}{\nu_2} \right) = C^2 G \int_{\nu_1}^{\nu_2} \frac{S_\nu}{\nu^2} d\nu$$

where C is the speed of light and G = 2.5db (linear) with $\nu_1 = 2\text{GHz}$ and $\nu_2 = 17\text{GHz}$.

f. Dependence of RF Emission on Voltage

The final measurements of emitted RF from the thruster were made with the intention of determining what dependence the maximum magnitude of the RF noise has on initial capacitor voltage and stored energy. Since the noise is all generated at the instant electrical breakdown is initiated between the electrodes it was reasoned that there should be no energy dependence of the emitted noise. That is, only a very small fraction of the total stored capacitor energy is deposited during the time period over which the noise is generated. It seemed more logical for the magnitude of the noise spikes to be related to the initial voltage on the electrodes if indeed a dependency on any of the initial conditions existed at all. Two sets of data were taken to either prove or disprove this hypothesis. The first set involved varying the initial voltage on a capacitor bank of fixed capacitance and measuring the maximum generated noise at each voltage. The second set of measurements consisted of varying the initial voltage at constant stored energy by varying the capacitance such that $C_1 V_1^2 = C_2 V_2^2 = C_3 V_3^2$, etc. Both sets of data were obtained using a power supply to provide the charge.

The data were plotted on log-log paper with the Poynting flux per unit frequency S_ν the ordinate and V_0 the abscissa. At values of V_0 for which two or more sets of data were available the values of S_ν were averaged. A strong power law dependency of S on V_0 was immediately apparent (see Figure 27). To determine the best fit of the data least mean squares fits (LMS) of the relationships $S = AV^p$ and $S = BV_0^q E_0^r$ were made. The latter fit was made so that if indeed an energy dependence did exist it could be discovered. The LMS fits yielded the following expressions:

$$S_\nu(V_0) = 6.859 \times 10^{-14} V_0^{3.687} \text{ mW/m}^2/\text{MHz (at 1m)}$$

$$S_\nu(V_0, E_0) = 3.11 \times 10^{-14} V_0^{4.385} E_0^{-.923} \text{ mW/m}^2/\text{MHz (at 1m)}$$

with V_0 in volts and E_0 in Joules. Both relationships indicate increasing radiation flux with increased initial voltage. Note that since $E_0 = 1/2 CV_0^2$ the second relationship can be rewritten as

$$S_\nu(V_0, C) = 4.4 \times 10^{-14} V_0^{2.539} C^{-.923} \text{ mW/m}^2/\text{MHz (at 1m)}$$

which still shows that increasing the initial voltage increases the radiation flux.

Deviation of the data from the LMS fit assuming only voltage dependence is larger than when both voltage and energy are taken as independent variables. This can be seen by comparing Figure 27 to Figure 28 where $S_\nu E_0^{.923}$ is plotted versus V_0 . Quantitatively, the average deviation of all data points assuming $S_\nu(V_0)$ is 27% as opposed to 15% for $S_\nu(V_0, E_0)$. Thus, it would appear that there is a real dependency of S_ν on initial energy, but physical reasoning contradicts this.

An additional point concerning these data fits which bears mentioning is the fact that Thomassen's data (taken on a 16J engine at 1430VDC at 0.666m from the source) agrees more closely with the value which would be predicted by the $S(V_0)$ fit than that predicted by the $S(V_0, E_0)$ fit. Thomassen gives a source strength of 10 to 60 mW/GHz assuming a source gain of 2. Using this source gain the relationship $S(V_0)$ predicts a value of 185mW/GHz at 1430V, whereas the $S(V_0, E_0)$ fit yields 1036mW/GHz. Furthermore, taking the actually measured value of S_ν at 2740V as opposed to arbitrarily using a value of 1430V into the fitted relationship yields a predicted source strength of 32mW/GHz when reduced to 1430V.

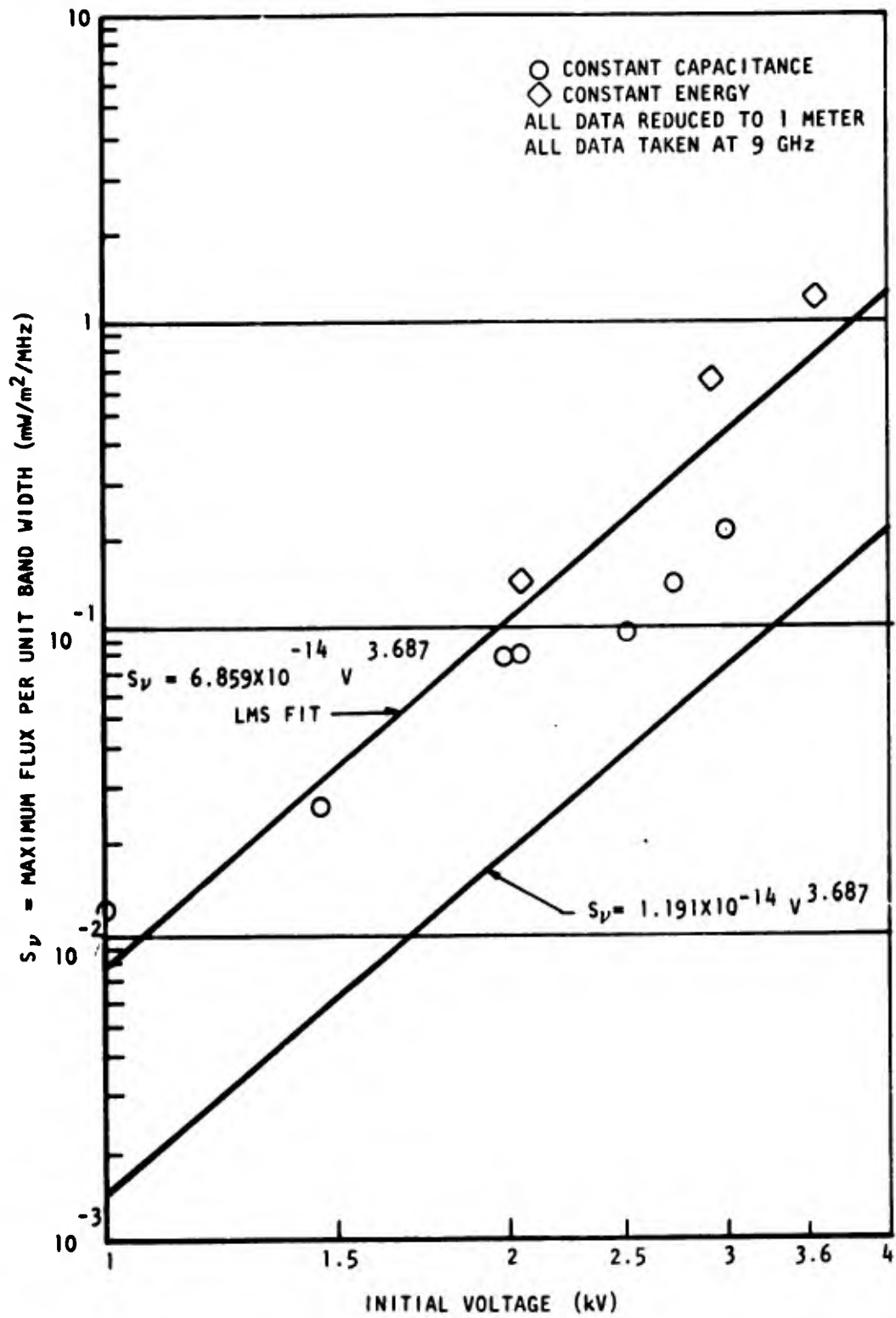


Figure 27 Poynting Flux Vs Initial Voltage

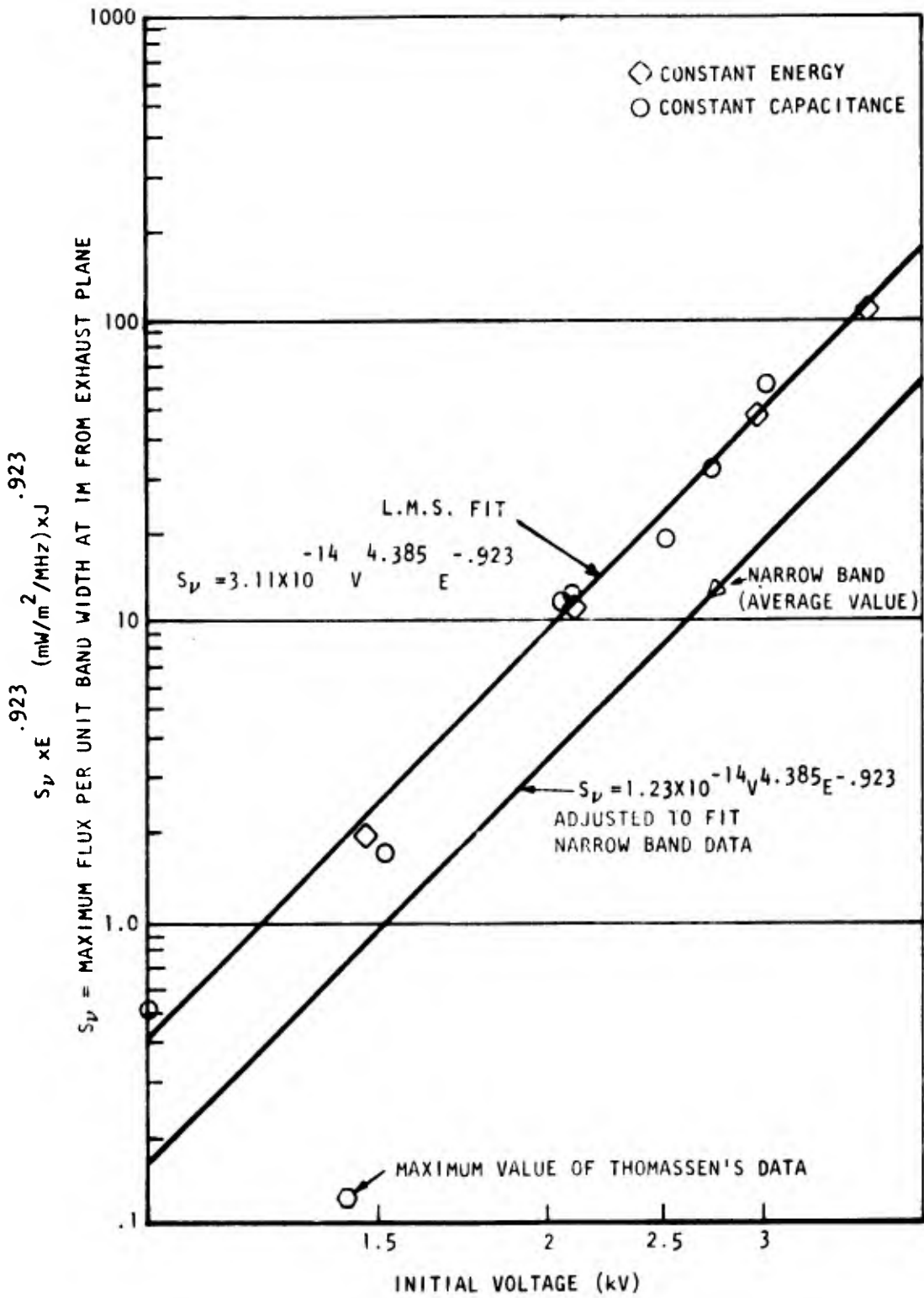


Figure 28. Poynting Flux Vs, Initial Voltage and Energy

Following the same procedure using the voltage-energy fit results in a predicted strength of 408mW/GHz. In both cases using only voltage as the independent variable yields predicted values of source in strength which are made much closer to what Thomassen actually measured than obtained by assuming both voltage and energy to be independent variables.

It should be noted that the value of S_V calculated from either the voltage or voltage-energy data fits is higher than that actually measured at 2740V. The calculated source strength based on our measurements at 2740 is 355mW/GHz. The LMS fits predict values of 901 and 2039mW/GHz using $S(V_0, E_0)$ and $S(V_0)$; respectively.

4. POSSIBLE EFFECTS OF ENVIRONMENT ON MEASURED RADIATED RF

The data on radiated RF presented herein was taken over a significant length of time. During this period certain qualitative observations regarding these measurements were made. These observations concern the effect of environmental conditions on the measured radiated RF which may have a bearing on the values and even the frequency of the emissions.

The narrow band data was taken over a long interval with the thruster under vacuum conditions most of the time. There were occasions when the vacuum chamber was vented to atmosphere and opened for one reason or another. After immediate re-evacuation the thruster appeared to be much noisier to the extent that large noise spikes were observed more frequently and there was considerable hash on the received signals. After running several hundred discharges the frequency of observation of large spikes was significantly reduced. It is well known that outgassing occurs during the initial firings of the thruster. This has been confirmed by measurements of the weight change of the electrodes and fuel immediately after removal from a vacuum chamber and reweighing after a few hours in air [9]. These effects have also been indirectly inferred from thrust measurements on thrusters which have been fired immediately after pumping down. The thrust measurements are high initially and come down to a steady value after a few hundred discharges. For this reason thrust measurements are never taken during the first few hundred discharges after pumping down.

It is believed that early measurements are therefore not representative of the true radiated RF in vacuum because of the presence of entrained material on the electrode surfaces. A large amount of variability is also evidenced by the difficulty encountered in getting some of the narrow band data. During some of these measurements the RF pulse level all but went to zero. Data were not taken at these times since these events were considered to be peculiar compared to the normal pattern of the pulse amplitude with the number of firings.

No quantitative explanation for these observations is available at this time since the processes producing the RF are not known. It is believed that the variability we have described is associated with the surface conditions of the electrodes. These conditions are influenced by vacuum chamber conditions (i. e. , backstreaming of diffusion pump oil) and gas absorption at the electrode surfaces after opening the chamber.

VI. SAFETY CONSIDERATIONS

1. SYSTEM SAFETY

There are two aspects of the pulsed plasma propulsion system which could lead to injury of personnel during handling if the proper procedures are not adhered to. The first of these is the main discharge capacitor bank. Capacitors have a tendency to accumulate charge via dielectric absorption if they are not shorted while lying in an ambient state. Thus, whenever the thruster is transported or taken off test for one reason or another a shorting cable with alligator clips on each end should be placed between the thruster anode and cathode and should be the last item removed prior to placing the thruster system on test. Similarly, the 2 microfarad capacitor bank in the discharge initiating circuit should also be shorted when not in use. This can be done by shorting the 620V input cable leading to these capacitors.

The other characteristics of this system requiring care in handling are the negator springs used to feed the propellant rods. These springs will snap violently if released at one end from their extended condition. They have extremely sharp edges and can lead to serious injury if this occurs. A definite procedure involving the use of C-clamps is followed when loading or unloading the feed system for assembly and disassembly of the thruster. This procedure is lengthy and a knowledgeable representative of Republic should be consulted if the need for disassembly arises.

In addition to the above, this particular thruster utilizes BeO for heat conduction from the electrodes to the radiators. This material is extremely toxic and even small traces, whether inhaled as dust or ingested, can be fatal. Hence, no rework of these slabs should be attempted. Moreover, should a slab fracture or break it should not be handled because of small particles which might be picked up and later ingested. If for any reason a slab is broken no attempt should be made to repair it, and Fairchild Republic shall be notified immediately.

Possible resulting damage may occur if caution is not exercised with the following:

1) never attempt to fire the thruster in air under normal atmospheric conditions or at a vacuum pressure above 10^{-4} mm Hg, and 2) never supply power to the power converter unless there is a load on the high voltage output leads.

2. TEST FACILITY SAFETY REQUIREMENTS

Various safety switches must be incorporated to guard against accidental damage to the thruster during testing in a vacuum facility. These are outlined below.

- (i) A high pressure cut-off switch which shuts down all power going into the converter and also the triggering pulser if the chamber pressure rises above 8×10^{-4} mm Hg.**
- (ii) Separate on-off switches on the hot side of the 28VDC input to the power converter and on the trigger line.**
- (iii) A dump circuit consisting of a 500 ohm resistor in series with a high-voltage (3kV) DPDT relay. One side of this relay is left open and the other is connected across the high voltage output of the converter with the resistor in series. When activated the relay should be in the open position and when deactivated the relay should close the path between the converter and resistor. This switch is used for manual emergency shut-down of the thruster and must be situated outside the vacuum chamber.**
- (iv) No AC current must be allowed to flow inside the chamber while the thruster is firing.**

VII. CONCLUSIONS AND RECOMMENDATIONS

The objectives set for this program required several advances in state-of-the-art technology. These were outlined in the Introduction to this report. Each of those areas of technical progress required to meet program objectives involved a major subsystem of the thruster; namely, the capacitors, power converter, and propellant storage geometry and feed mechanisms.

Extensive testing, research, and development efforts carried out at Fairchild Republic during this program have resulted in making the side-fed electrode/propellant geometry and its associated high performance level a reality. A multiplicity of problems associated with feeding propellant from the sides have been encountered and solved. Helical shaped propellant rods divided into three separate individually fed sections across their width were fabricated and the associated feed mechanism was developed and tested. Details of the nozzle design and electrical interfacing between subsystems have been generated as part of developmental testing. The basic thruster configuration meets the objectives set for volume and weight. Specific impulse (1794s) and thrust efficiency (31.5%) both exceed the values set as goals and a capability of 38.284 lbs exists with the thruster in its current configuration. Overall system efficiency falls somewhat short of the 26.7% goal by about 1%.

A breadboard power converter using the fly-back technique for capacitor charging from a DC source was fabricated by Wilmore Electronics Co., Inc. This converter was tested with the thruster and met all Republic specifications. The converter is 80.4% efficient at 2740VDC output and 81.4% efficient at 2500VDC.

High energy density capacitors (40J/lb = 88J/kg) were built by Capacitor Specialists, Inc. Problems arising because of oil leakage in a vacuum environment from these capacitors did not allow a full assessment of their life capability and life testing the thruster system was not possible because of this. Technology does exist at this time to insure a hermetically sealed oil impregnated capacitor, as evidenced by the efforts of Massachusetts Institute of Technology Lincoln Laboratory in procuring their capacitors for the LES-9 thrusters [10] from CSI. It is clear that the highest standards of quality control and assurance must be applied through out the fabrication of such capacitors if high reliability is to be guaranteed. It is not known whether the leakage problems experienced on this program were the result of rework which had to be done by CSI so that they would conform to the terminal geometry in Republic's procurement specification, and there is no way to tell what the results would have been if the specification was adhered to during the initial fabrication or if the rework was not done.

On the basis of radiated RF measurements made on the thruster during this program the following conclusions can be made:

- (i) The RF signal emitted from pulsed plasma thrusters is broadband impulse type noise.
- (ii) The RF is emitted at the instant of breakdown between the electrodes in the form of a spike having a width of from 100 to 300ns and an amplitude whose magnitude follows a nearly random distribution from zero to maximum. The rise time is on the order of 10ns.
- (iii) The maximum amplitude of the RF spike is directly proportional to a power of the initial voltage on the electrodes. There may also be an inverse dependence on the initial stored energy but the radiation flux is more likely proportional to the rate of energy input to the arc at discharge initiation.
- (iv) The effect of the exhaust cone is to scatter RF energy into the forward direction.

Future investigations should be carried out to generate the following information:

- (i) Amplitude and spectrum of conducted RF on the power input and trigger pulse leads.
- (ii) The effects of the time varying electromagnetic fields on electronic components within the spacecraft. This type of testing would involve simulation of the spacecraft shell and instrumentation to determine if there are voltages induced as a result of thruster firing.
- (iii) The effect of gas and oil vapor absorbed on the electrodes on the amplitude of the noise signal.

At this time the basic thruster hardware required to meet mission requirements is available. The only components necessary to prove the system out in an endurance test are reliable energy storage capacitors. It is recommended that such testing be initiated as soon as possible even if this requires using a bank of capacitors which is heavier than optimal. Doing this would allow evaluation of the thruster components on a long term basis and provide an opportunity to encounter any potential operational problems which may still exist. Such a test would also allow generation of data concerning conductive EMI along the power input leads and the trigger pulse leads.

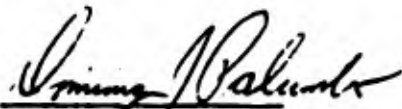
The prognosis for generating a bank of high energy density capacitors meeting the required life and weight appears better at this time than it appeared prior to program initiation. Having generated encouraging thermal-vacuum and performance data has yielded more credibility concerning the use of KF-film capacitors for this application. The technology necessary to insure hermetically sealed units being available, it is essential that those procedures be followed. Capacitor cans must be hydroformed or deep drawn to insure homogeneity and dimensional uniformity. High voltage bushing assemblies and ground rings must be vacuum brazed onto the cans and helium leak tested to insure the seals. The back lid, usually soldered in place after placing the winding into the can, must be redundantly sealed by electron beam welding after impregnating the capacitor with oil. Impregnation should be done under conditions which place the impregnant under positive pressure when brought back to standard atmospheric conditions. The filler hole plug is generally soldered in place after impregnation. A redundant seal should be provided to insure a leak tight seal around the filler plug area.

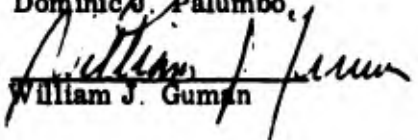
REFERENCES

1. Palumbo, D. J. , and Guman, W. J. ; Pulsed Plasma Propulsion Technology, Interim Report, AFRPL - TR-73-79, Sept. 1973.
2. Guman, W. J. ; Development of a Short Pulsed Solid Propellant Plasma Thruster, Final Report MS172R0001, Mar. 1974.
3. Dailey, L. , and Davis, H. ; Pulsed Plasma Technology Final Report, AFRPL - TR-73-81, July 1973.
4. Palumbo, D. J. and Guman, W. J. ; Propellant Sidefeed - Short Pulse Discharge Thruster Studies, NASA CR-112035, Jan. 1972.
5. Kalygin, A. G. , et. al. ; Energy Characteristics of a Pulsed Dielectric-Erosion Plasma Accelerator, Sov. Phys. Tech. Phys. , 15 , 6, Dec. 1970.
6. KREHA Chemical Industry Co. , Std; Application of KREHA KF-Film to Capacitors, Properties Bulletin.
7. Thomassen, K. I. ; Radiation from Pulsed Plasma Thrusters, AIAA Paper 73-263, Jan. 1973.
8. Volk, W. ; Applied Statistics for Engineers, McGraw Hill, 1958.
9. Guman, W. J. , and Truglio, W. ; Surface Effects In a Pulsed Plasma Accelerator, AIAA J. , 2 , 7, July 1964.
10. Vondra, R. and Thomassen, K. ; A Flight Qualified Pulsed Electric Thruster for Satellite Control, AIAA Paper 73-1067, Nov. 1973.

APPENDIX A

PRODUCT SPECIFICATION FOR:
WILMORE ELECTRONICS
POWER CONDITIONER FOR
PULSED PLASMA THRUSTER

Prepared by: 
Dominic J. Palumbo

Approved by: 
William J. Guman

1.0 SCOPE

This tentative specification describes an energy conversion scheme specifically designed for a Pulsed Plasma Thruster.

2.0 REQUIREMENTS, GENERAL

The power conditioner shall perform the function of accepting a low DC voltage and charging two capacitor loads to predetermined high voltages without warm-up time. The primary objective is to perform this energy conversion process as efficiently as the state-of-the-art permits. While the system shall be substantially of "bread-board" type of construction, requirements and goals specified herein shall be met.

The design of the power conditioner shall be such that, optionally, at a later date it will be possible for Wilmore Electronics to perform minor modification such that the main output voltages can be changed as specified herein.

3.0 INPUTS

3.1 Primary Power

Primary power to the power conditioner will be supplied by a 28 VDC laboratory power supply. The input voltage can vary over the range 28 ± 2 volts.

3.2 Housekeeping

The power conditioner will be "on" when the 28 ± 2 volt primary power is applied and "off" when the 28 ± 2 volt power is removed.

4.0 OUTPUTS

4.1 Option 1

Under Option 1, the power conditioner shall be capable of charging a 240 ufd $\pm 10\%$ capacitor such that one terminal of the capacitor shall be - (minus) 1250 volts DC and the other terminal of the capacitor to + (plus) 1250 volts DC with respect to the power conditioner ground reference. The 2500 volts differential shall be within $\pm 2\%$.

4.2 The power conditioner shall also supply an output capable of charging a 2.0 ufd $\pm 5\%$ capacitor to + (plus) 620 volts DC in unison with the voltages of paragraph 4.1.

4.3 Option 2

Under Option 2, the power conditioner when appropriately modified by Wilmore Electronics shall be capable of charging a 240 ufd $\pm 10\%$ capacitor such that one terminal shall be at 0 volts (negative ground) and the other terminal at + (plus) 2500 volts DC with respect to the negative ground reference. The 2500 volts differential shall be within $\pm 2\%$.

4.4 The power conditioner shall also supply an output capable of charging a 2.0 ufd $\pm 5\%$ capacitor to + (plus) 620 volts DC in unison with the voltage of paragraph 4.3.

4.5 The power conditioner output will have a guaranteed minimum average energy delivery rate of 111 J/S under the most severe operating environment.

5.0 DUTY CYCLE

The pulse rate will be adjusted to deliver 111W of average power to the capacitors at full maximum charge of 2500V $\pm 2\%$. When the load capacitors are charged, the power conditioner high voltage outputs must be maintained with $\pm 2\%$ for the 2500 volt differential of either Option 1 (paragraph 4.1.4.2) or Option 2 (paragraph 4.3.4.4) and 620 ± 20 volts until the capacitor loads are discharged. If the 620 volt output should be discharged while the 2500 volt differential has not, both the 620 and the 2500 voltage differential shall be restored in the next charge cycle.

6.0 PROTECTION

6.1 Short Circuit Protection

The power conditioner shall not sustain damage when operating into a short circuit in any of the load capacitors for sustained periods.

6.2 Bleeders

In the event that any of the output loads of the power conditioner fail (s) to be discharged following removal of the 28 volt primary power, the 2500 volt differential will be discharged through bleeders to less than 70 volts in 2 hours or less.

7 0 ENVIRONMENTAL CONDITIONS

7.1 Pressure

The power conditioner shall be required to operate as specified when the ambient pressure is less than 10^{-4} Torr. The power conditioner will not be operated in the pressure range from 10^{-4} Torr to atmospheric pressure. Operation at atmospheric pressure shall be possible.

7.2 Temperature

The power conditioner shall be required to operate as specified when exposed to vacuum conditions with the temperature of the mounting structure in the 0 F to 140 F as a steady state temperature or cycling between these limits with a period greater than 6 hours.

8.0 EFFICIENCY OF ENERGY CONVERSION

The required energy conversion efficiency defined as

$$\frac{\text{output}}{\text{input}} = \frac{CV^2}{\int V i dt}$$

i. e. , the energy on the capacitor loads divided by the input power integrated over the charge cycle shall be guaranteed to be an absolute minimum of 82% with a goal of 86% or better.

9 0 CONNECTORS

Both the input and output connectors shall be by insulated standoffs appropriately marked. Soldering to these standoffs shall be possible without damage of the power conditioner. Location of the connectors shall be as per mutual agreement between Wilmore Electronics and Fairchild Republic.

10 0 EMI

Conducted EMI on the input power bus shall be kept as low as possible. EMI line filtering shall be provided to meet this objective. The enclosure of the power conditioner shall be fabricated to prevent radiated EMI from the power conditioner. Pro-

visions shall be made to the enclosure around the output terminal to enable the output terminals to be enclosed by Fairchild Republic while interfacing the power conditioner to the thruster.

11.0 NOISE SUSCEPTIBILITY

Operation of the power conditioner shall not be disturbed nor performance degraded when it is subjected to RF fields in the VHF-UHF band of as much as one volt/meter adjacent to the power conditioner.

12.0 WEIGHT

While maximum efficiency is the primary requirement of the power conditioner system weight shall be kept as low as reasonable without affecting efficiency requirements or life requirements. As a goal the power conditioner shall weigh no more than four (4) pounds.

13.0 LIFE

The power conditioner shall function as specified herein for at least 10^8 cycles.

14.0 DIMENSIONS

The extreme outside dimensions of the power conditioner shall not exceed the following envelope:

8.5 inches x 3 inches x 11 inches

15.0 DOCUMENTATION

An informal monthly progress letter shall be sent to Fairchild Republic.

16.0 MOUNTING PROVISION

The power conditioner shall be supplied with mounting provisions to be mutually agreeable to Wilmore Electronics and Fairchild Republic.

18 August 1973

Wilmore Electronics Co , Inc.
P.O Box 2973
Durham, N. Carolina 27705

Attention: Mr. D. Cox

Dear Don:

This is to formalize our requirement for 2740 $\pm 2\%$ volts charging 200 microfarads of capacitance on the output of the power converter not being constructed under Spec MS14730002. Please make the following changes in that specification:

Paragraph 4.1

Change "240 microfarads $\pm 10\%$ " to "200 microfarads $\pm 5\%$ "
Change "- (minus) 1250 VDC" to "- (minus) 1370 VDC"
Change "+ (plus) 1250 VDC" to "+ (plus) 1370 VDC"

Paragraph 4.3

Change "240 microfarads $\pm 10\%$ " to "200 microfarads $\pm 5\%$ "
Change "+ (plus) 2500 VDC" to "+ (plus) 2740 VDC"

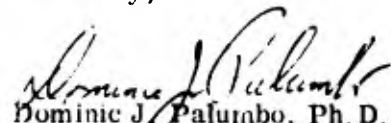
Paragraph 5.0 and 6.2

Change "2500 Volt" to "2740 Volt"

Sorry for these changes at this late date, but our capacitor manufacturer has come in out of Spec on capacitance and we must maintain the energy at 750J to satisfy contract requirements.

Thanking you for your accommodation, I am


Sincerely,

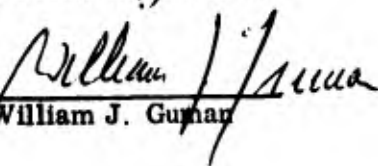

Dominic J. Palumbo, Ph. D.
Project Engineer

DJP:mz

APPENDIX B

PRODUCT SPECIFICATION
FOR
CAPACITOR SPECIALISTS, INC.
ENERGY STORAGE CAPACITOR
MODEL 3K125TN

Prepared by: 
Dominic J. Palumbo

Approved by: 
William J. Gunnar

1.0 SCOPE

This specification describes and establishes requirements for a fixed, liquid impregnated energy storage capacitor specifically tailored for the solid propellant pulsed plasma thruster. The capacitor shall be designated as the CSI Model 3K125TN capacitor.

2.0 REQUIREMENTS

2.1 Capacitance

60.0 microfarads $\pm 5\%$ when measured at +25 C and 60 Hz.

2.2 Rated Voltage

2500 VDC

2.3 Design Life

The capacitor shall be designed for a life of 10^7 discharges with a guaranteed lifetime of 6×10^6 discharges into a plasma load characterized by the following current and voltage traits:

- 1) Maximum Current -- 25,000 A
- 2) Initial Rate of Current Increase -- 3.0×10^{10} A/sec
- 3) Maximum Voltage Reversal -- 25%
- 4) Approximate time averaged load impedance -- 4-6 milliohms

2.4 Operating Temperature Range

-35 C to 45 C maximum

2.5 Dissipation Factor

.013 measured at +25 C to 60 Hz

2.6 Energy Density

Guaranteed minimum of 40 Joules/pound at rated voltage.

3.0 CONSTRUCTION

The capacitor shall conform to the design and construction requirements specified herein

3.1 Dielectric

K-film (Kureha Polyvinylidene Fluoride PVD) - Paper, Castor Oil Impregnant

3.2 Terminals

A center (positive) stud and ground ring in the configuration shown in Figure 1 shall be supplied.

3.3 Geometry and Physical Dimensions

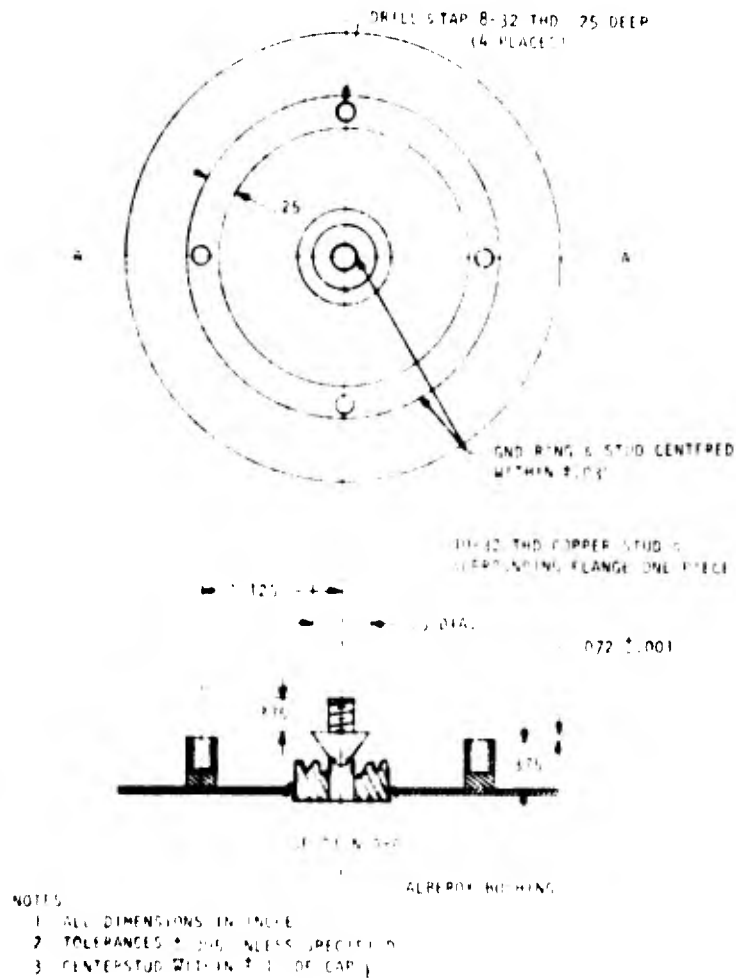


Figure 1. Terminal Geometry

The external physical dimensions shall be as specified in Figure 2.

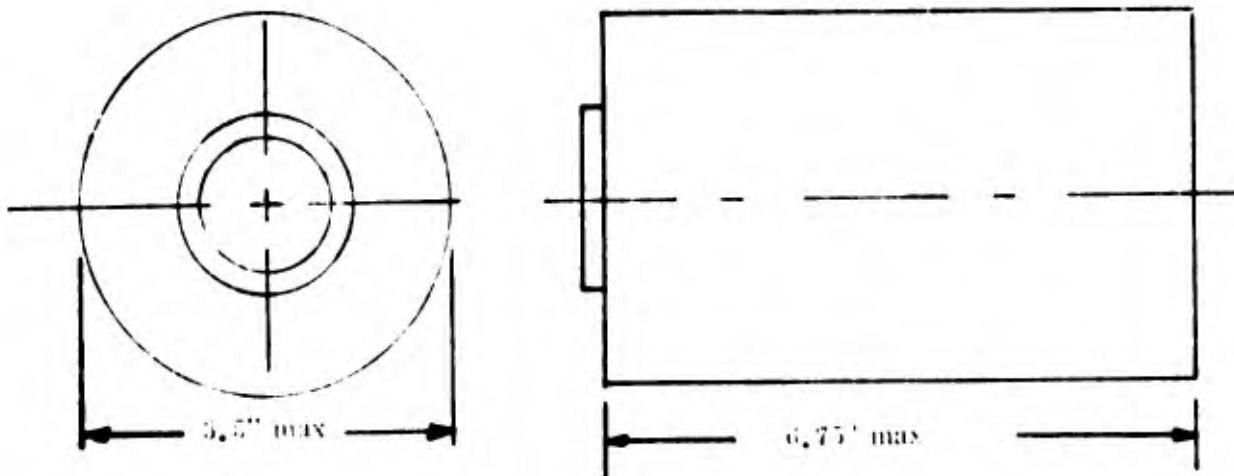


Figure 2. Geometry of Capacitor

4.0 SCREENING PROCEDURE

4.1 Testing Requirements

4.1.1 Capacitance

At + 25 C the capacitors shall be tested as follows:

Test Frequency - 1000 ± 100 Hz

Requirement - The capacitance shall measure 60 microfarads $\pm 5\%$
(57 microfarad minimum and 63 microfarad maximum)

The data shall be recorded and supplied to Fairchild Republic Company on delivery of the capacitors.

4.1.2 Dissipation Factor

At +25 C the dissipation factor shall be measured at an AC voltage of 1 volt at a frequency of 1000 ± 100 Hz, and at 300 VAC at 60 Hz. The dissipation factor shall not exceed .013 in either case. The data shall be recorded and submitted to Fairchild Republic on delivery of the capacitors.

4.1.3 High Voltage Standoff in Vacuo

The capacitor shall be placed in vacuo after potting at a pressure of 50 microns for a period of twenty-four (24) consecutive hours. The capacitor shall be placed in the vertical position with studs facing upwards during this time. At the completion of vacuum soak a voltage of 3500 VDC will be applied and maintained for one (1) minute. There shall be no momentary or intermittent arcing or other indication of breakdown, nor shall there be any visible evidence of damage.

4.1.4 Repetitive Arc Discharge Capability

The capacitors shall be repetitively discharged for 500 cycles into an arc discharge simulator to be supplied by Republic for testing purposes. Capacitors shall be charged to 2500 VDC and discharged once every 6.75 sec.

4.2 Test Witness

A representative of Fairchild Republic shall be present when the tests outlined in Sections 4.1.3 and 4.1.4 are carried out.

4.3 Certification

A certificate of compliance to the specification presented herein shall be provided with each capacitor.

4.4 Marking

Marking shall be provided in accordance with manufacturers usual procedure.

4.5 Guarantee

The vendor shall assume the expense of repairing any unit that has not met the guaranteed lifetime specified herein if a failure analysis indicates the failure to be a material or fabrication fault.